

Please cite the Published Version

Allen, Norman S., Edge, Michele, Verran, Joanna, Caballero, Lucia, Abrusci, Conception, Stratton, John, Maltby, Julie and Bygott, Claire (2009) Photocatalytic surfaces: environmental benefits of Nanotitania. *The Open Materials Science Journal*, 3. pp. 6-27. ISSN 1874-088X

DOI: <https://doi.org/10.2174/1874088X00903010006>

Publisher: Bentham Open

Version: Published Version

Downloaded from: <https://e-space.mmu.ac.uk/70794/>

Usage rights:  [Creative Commons: Attribution-Noncommercial 3.0](https://creativecommons.org/licenses/by-nc/3.0/)

Additional Information: This is an Open Access article which appeared in *The Open Materials Science Journal*, published by Bentham Open

Enquiries:

If you have questions about this document, contact openresearch@mmu.ac.uk. Please include the URL of the record in e-space. If you believe that your, or a third party's rights have been compromised through this document please see our Take Down policy (available from <https://www.mmu.ac.uk/library/using-the-library/policies-and-guidelines>)

Photocatalytic Surfaces: Environmental Benefits of Nanotitania[§]

Norman S. Allen^{*,1}, Michele Edge¹, Joanne Verran¹, Lucia Caballero¹, Concepcion Abrusci², J. Stratton³, Julie Maltby³ and Claire Bygott³

¹Biology, Chemistry and Health Sciences, Manchester Metropolitan University, Chester Street, Manchester M1 5GD, UK

²Visiting Fellow, UCM, Madrid, Spain

³Millennium Chemicals, P.O. Box 26, Grimsby, N.E. Lincs, DN41 8DP, UK

Abstract: The use of photocatalytic titania nanoparticles in the development of self-cleaning and depolluting paints and microbiological surfaces is demonstrated. In the former case surface erosion and sensitised photooxidation is shown to be controlled by the use of catalytic grades of anatase nanoparticles. For environmental applications in the development of coatings and cementitious materials for destroying atmospheric pollutants such as nitrogen oxides (NOX) stable substrates are also illustrated with photocatalytic nanoparticles. Here porosity of the coatings through calcium carbonate doping is shown to be crucial in the control of the effective destruction of atmospheric NOX gases. Good environmental stability of the coatings is also crucial for long term durability and this aspect is examined for a variety of material substrates. For the development of microbiological substrates for the destruction of harmful bacteria/fungi effective nanoparticle anatase titania is shown to be important with hydrated high surface area particles giving the greatest activity. Data from commercial pilot studies is used to signify the important practicalities of this type of new technology.

Keywords: Nanoparticles, pigments, titanium dioxide, anatase, rutile, de-pollution, self-cleaning, cementitious, photocatalysis, anti-bacterial, paints, coatings.

INTRODUCTION TO PHOTOCATALYSIS: TITANIUM DIOXIDE CHEMISTRY AND STRUCTURE-ACTIVITY

For many years, titanium dioxide pigments have been used successfully for conferring opacity and whiteness to a whole host of different materials. Their principal usage is in such applications as paints, plastics, inks and paper but they are also incorporated into a diverse range of products, such as food and pharmaceuticals. The fundamental properties of titanium dioxide have given rise to its supreme position in the field of white pigments. In particular, its high refractive index has enabled the efficient scattering of light. Its absorption of ultraviolet light has conferred durability to products. Its non toxic nature has meant that it can be widely used in almost any application without risk to health and safety. However, the primary reason for its success is the ability to reflect and refract, or scatter light more efficiently than any other pigment, due to its high refractive index in comparison with extenders, fillers, and early pigments [1-5].

Titanium dioxide exists in three crystalline modifications, rutile, brookite, and anatase, all of which have been prepared synthetically. In each type, the titanium ion coordinates with six oxygen atoms, which in turn are linked to three titanium atoms, and so on. Anatase and rutile are tetragonal while brookite is orthorhombic. Brookite and anatase are unstable

forms. Brookite is not economically significant since there is no abundant supply in nature.

During the manufacturing process of TiO₂, the pigment is formed as discreet particles of around 0.2-0.4 microns. The titanium dioxide manufacturers control the operation variables to produce particles of a uniform size and distribution. These 0.2-0.4 micron particles have been engineered to maximize the scattering of light, resulting in optimum brightness and opacity.

However, as soon as the particles are manufactured, they begin to combine into aggregates, agglomerates, and flocs. *Aggregates* are associations of pigment particles that are fixed together along the crystal faces. Bonds between particles are strong and cannot be broken by conventional grinding devices. *Agglomerates* are associations of pigment particles and aggregates that are weakly bonded together. *Flocs* are associations of crystallites, aggregates, and agglomerates joined across corners or held together by short range attractive forces. These flocs disperse under moderate shear

Aggregates can only be broken into individual pigment particles with intensive milling. One of the last manufacturing steps performed by the TiO₂ manufacturer is micronization and/or milling to dissociate as many aggregates as possible. Aggregates will not reform unless the pigment is heated to over 500°C. Agglomerates are also broken up in the milling step. However, agglomerates will easily reform during packing, storage and transportation. The disruption of these inter-particle bonds is generally understood to be the dispersion that needs to be performed by the TiO₂ consumer.

*Address correspondence to this author at the Biology, Chemistry and Health Sciences, Manchester Metropolitan University, Chester Street, Manchester M1 5GD, UK; E-mail: N.S.Allen@mmu.ac.uk

[§]Presented at NanoFun Congress April ROMA 2008.

It is possible to manipulate TiO₂ particle size to within a very narrow range around a predetermined optimum. Generally, in paint applications this optimum is approximately 0.2-0.3 microns, for it is within this range that TiO₂'s light scattering ability is at its peak, which in turn maximises the level of gloss finish.

TiO₂ pigment particles are submicroscopic with size distributions narrower than many so-called monodisperse particulates. Appropriately ground, pigment dispersions contain less than five weight percent of particles smaller than 0.10 microns and larger than 1.0 micron. Optical effectiveness, that is, light scattering is controlled by the mass/volume frequency of particles in the size range from 0.1 to 0.5 microns. Gloss is diminished by a relatively small mass/volume fraction of particle larger than about 0.5 microns. Dispersability and film fineness is degraded by a very small mass/volume fraction of particles larger than about 5 microns. Important optical properties like opacity, hiding power, brightness, tone, tinting strength and gloss are all dependent upon the particle size and particle size distribution.

Pure titanium dioxide possesses by nature an internal crystal structure that yields an innately high refractive index. When the particle size and particle size distribution is to be optimised so as to contribute along with its high refractive index to a maximum light scattering, conventional or pigmentary titanium dioxide is obtained. It reflects all the wavelength of the visible light to the same degree, producing the effect of whiteness to the human eye. All these attributes, together with its opacity, are achieved for an optimal particle diameter which is approximately 0.2 to 0.4 microns, that is, in the order of half the wavelength of visible light. This fact can also be demonstrated on the basics of Mie theory [6].

There exists, however, another type of titanium dioxide whose median crystal size has been explicitly reduced up to 0.02 microns. This is the so called nanoparticles or ultrafine TiO₂ and will be the subject matter of this article.

The history of nanoparticle titanium dioxide dates back to the late 70's when the first patent on the preparation of these materials was issued in Japan. It is in principle possible to obtain nanoparticle TiO₂ by simple milling of the pigmentary TiO₂ to a finer particle⁴. However, the properties of the fine powders in terms of purity, particle size distribution and particle shape remain highly unsatisfactory. Several wet-chemical processes were developed during the 80's by TiO₂ pigment manufacturers like Ishihara, Tioxide and Kemira. The first part of the process, the production of the nanoparticles base material uses after-washes titanium hydroxylate as the raw material. After subsequent process steps involving the decomposition of the hydroxylate crystal structure and the reprecipitation of the TiO₂, the product is calcined to obtain oval-shaped particles with a desired primary crystal size and narrow size distribution. The base crystals are coated in the after-treatment unit according to the requirements of the end-use. One of the primary tasks of the after-treatment is to ensure good dispersability of extremely fine particles in the final application.

TiO₂ nanoparticles are also routinely produced by the gas-to-particle conversion in flame reactors because this method provides good control of particle size, particle crystal structure and purity [4].

Typically, the crystal size of these products is about a tenth of the size of the normal pigmentary grade. Fig. (1) shows typical TEM micrographs for pigmentary and nanoparticulate titanium dioxide at the same magnification.

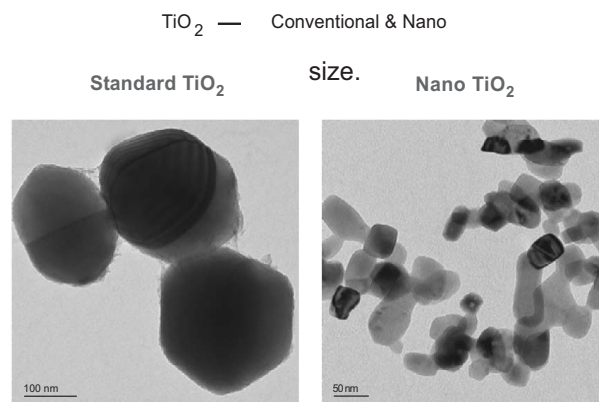


Fig. (1). Typical TEM Micrographs of pigmentary and nanoparticles.

The optical behaviour of ultrafine TiO₂ differs dramatically from that of conventional TiO₂ pigment. The optical properties of nanoparticle TiO₂ are governed by the Rayleigh theory of light scattering. A simple interpretation of this theory is that the shorter wavelengths of light are more efficiently scattered by very small particles. The intensity of the scattered light is inversely proportional to the fourth power of the wavelength. In practical terms, reduction in the crystal size of a TiO₂ product leads to an optimum size of TiO₂ of the order of 20-50 nm where the ultraviolet spectrum of light (200-400nm) is effectively scattered from the particles while the visible wavelengths are transmitted through the material. The material thus appears virtually transparent to the naked eye. The behaviour is demonstrated in Fig. (2), which shows the difference between pigmentary and nanoparticle TiO₂.

The complete picture of the optical behaviour of TiO₂ becomes more complete by recognizing that TiO₂ is a semiconductor. TiO₂ exhibits a characteristic energy gap of 3.23 eV or 3.06 eV between the valence band and the conduction band for anatase and rutile, respectively. Wavelengths shorter than 390 nm for anatase and 405 for rutile – corresponding to higher energy than the threshold energy – will excite electrons from the valence to the conduction band. Summarizing, titanium dioxide exhibits various mechanisms under exposure to light depending on the wavelength and the particle size: (see Table 1 and Fig. 3). Electron-hole pairs are formed giving rise to various sensitisation processes.

Based on the light scattering property described earlier, nanoparticle titanium dioxide can be used to impart excellent UV protection. Compared to the available UV absorbers, ultrafine nano-TiO₂ possesses effective UV filter properties over the entire ultraviolet spectrum (UVC + UVB + AVA). For example, it is gaining a wide acceptance for use in sun creams. Nanoparticle TiO₂, apart from its effective attenuating characteristics is extremely inert and therefore, safe to use next to the skin⁵. Nanoparticle TiO₂ can also be used in clear plastic films to provide UV protection to foodstuffs. UV radiation from artificial lighting in a grocery store induces autooxidation in e.g. meat and cheese, resulting in

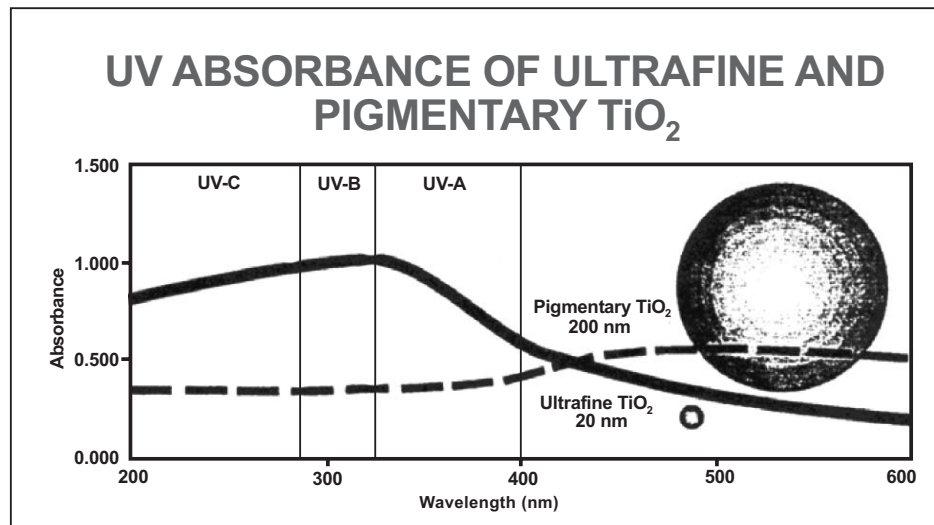


Fig. (2). Comparison of the optical behaviour of ultrafine TiO_2 and pigmentary TiO_2 .

discoloration. In this regard it also exhibits ant-bacterial behaviour which will be discussed later.

Table 1. Optical Behaviour of Pigmentary and Nanoparticle TiO_2 Under Visible and UV Light

Particle Size	Wavelength < 400	Wavelength > 400
Pigmentary TiO_2	<ul style="list-style-type: none"> Semiconductor absorption. 	<ul style="list-style-type: none"> Scattering and reflection. (Mie scattering)
Nanoparticle TiO_2	<ul style="list-style-type: none"> Semiconductor absorption. Scattering and reflection. (Rayleigh's theory) 	<ul style="list-style-type: none"> Transmission of light. Particle diameter \ll wavelength

It is also possible to use ultrafine TiO_2 as a light stabilizer in plastics to protect the material itself from yellowing and to retard the deterioration of the mechanical properties. A further example of the potential of nanoparticle TiO_2 as a UV filter is found in clear wood finishes. The original colour of wood panels can be retained by a clear lacquer made with 0.5-4 % nanoparticle TiO_2 [7]. In addition to preventing wood from darkening, ultrafine TiO_2 also enhances its life-time. An exciting and increasing popular application of the optical properties of ultrafine TiO_2 is found in automotive coatings where the ultrafine powder is used as an effect pigment in combination with mica flakes to create the so-called titanium opalescent effect. For UV protection applications, and due to the intrinsic photoactivity of TiO_2 pigments, mainly, *nanoparticle surface treated rutile* pigments are used. *Nanoparticle anatase TiO_2* finds applications in the field of photocatalysis.

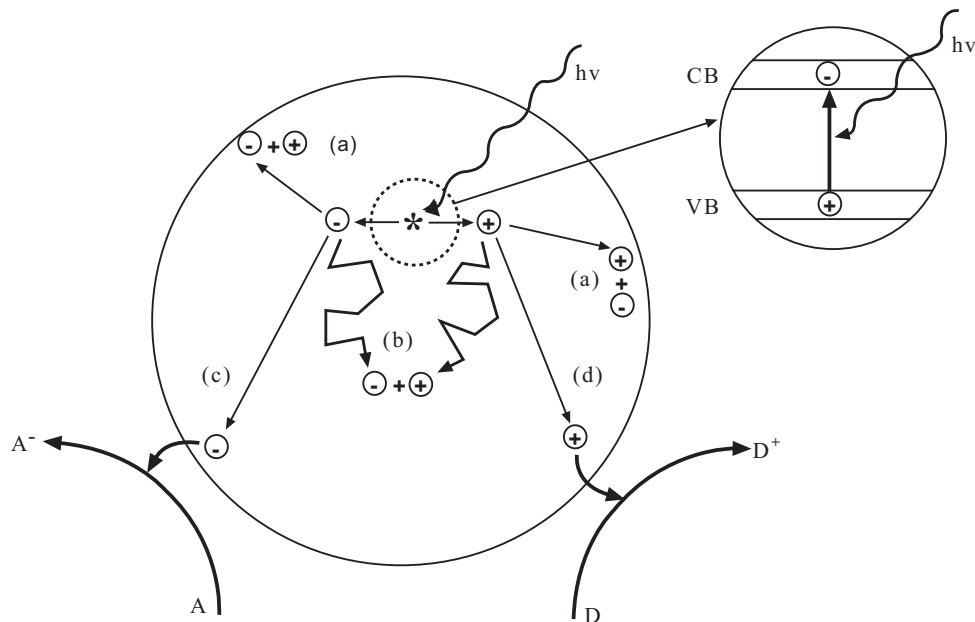


Fig. (3). Illustration of the major processes occurring on a semiconductor particle following electronic excitation. Electron-hole recombination can occur at the surface (reaction (a)) or in the bulk (reaction (b)) of the semiconductor. At the surface of the particle, photogenerated electrons can reduce an electron acceptor A (reaction (c)) and photogenerated holes can oxidize an electron donor D (reaction (d)). The combination of reactions (c) and (d) represent the semiconductor sensitisation of general redox reactions given later in the text.

APPLICATIONS

The field of heterogeneous photocatalysis is very diverse and involves many research groups throughout the world. A number of research themes have emerged which offer real potential for commercial developments and merit much greater research.

In this article we will focus on our application studies of TiO_2 for antibacterial, self-cleaning and depollution (Atmospheric contaminants such as VOC's and nitrogen oxides). For example, in indoor environments, most surfaces, e.g. ceramic tiles, windows glass or paper, are gradually covered with organic matter such as oils, dirt, and smoke residue and become fouled [8]. Transparent TiO_2 coatings can be completely unobtrusive, causing no readily discernable changes in the substrate colour or transparency, but they can decompose organic matter as it deposits. Thus, various types of surfaces with TiO_2 can be covered to make them self-cleaning under sunlight as well as room light. Thus, surfaces based on paints, ceramics, glass, cementitious materials containing active photocatalytic titania nanoparticles have widespread applications to create environmentally clean areas within their proximity.

PHOTOCATALYTIC CHEMISTRY

The overall catalytic performance of titanium dioxide particles has been found to be dependent on quite number of parameters including preparation method, annealing temperature, particle/crystal size, the specific surface area, the ratio between the anatase and rutile crystal phases, light intensity, and the substrate to be degraded [9]. Furthermore, the electrons confined in the nano-material exhibit a different behaviour from that in the bulk materials. The properties of the electrons in small semiconductors should be dependent upon the crystallite size and the shape due to quantized motion of the electron and hole in a confined space. This phenomenon is called the quantum size effect. But the quantization effect does not exist in amorphous phases [10]. As a result of the confinement, the band gap increases and the band edges shift to yield larger redox potentials. So the use of size-quantized semiconductor TiO_2 particles may result in increased photoefficiencies [11].

However, other workers [12] reported that the photocatalytic activity increased greatly and the blue shift was significant only at particle diameters less than 10 nm. On the other hand, the small size effect can improve the photocatalytic activity of the TiO_2 due to the increasing specific surface area which gives more reactive sites to absorb pollutants. Meanwhile, the diffusion of the photoinduced electrons or holes from bulk to surface becomes fast with a decrease in the particle size [13], which will also lead to an enhancement in the photocatalytic activity. On the other hand, the surface tension increases and causes a crystal lattice distortion with decreasing particle size [14] and consequent change in the structure of the energy band.

The TiO_2 anatase phase is more active than the rutile phase in photocatalysis. The reason for the lower photocatalytic efficiencies in the rutile TiO_2 phase is because the recombination of the electron-hole pair produced by UV irradiation occurs more rapidly on the surface of the rutile phase and the amounts of reactants and hydroxides attached to the

surface of the rutile phase are smaller than those of the anatase TiO_2 phase [15]. However, according to other work the decrease in the photocatalytic effect during the transformation from the anatase to rutile TiO_2 phase was not due to the change in the crystalline structure, but mainly due to changes in the specific surface area and porosity [16]. The photocatalytic processes on a titanium dioxide particle are displayed in Fig. (4). Primarily following photoexcitation a number of surface processes can take place providing activation and further reactions depending upon the nature of the environment in question. Holes can generate active hydroxyl radicals while active oxygen species are generated through electron transfer processes. All exhibit high activity that can react with surrounding organic and gaseous environments. The presence of alumina/silicate coatings for example, shown in this figure, will trap out surface generated electrons thus minimising the production of active surface species.

Polymeric and organic coatings systems are commonly utilised by titania doping for various applications. In outdoor applications all polymers degrade. The degradation rate depends on the environment (especially sunlight intensity, temperature and humidity) and on the type of polymer. This so-called photooxidative degradation is due to combined effects of photolysis and oxidative reactions. Sunlight photolytic degradation and/or photooxidation can only occur when the polymer contains chromophores which absorb wavelengths of the sunlight spectrum on earth (>290 nm). These wavelengths have sufficient energy to cause a dissociative (cleavage) processes resulting in degradation.

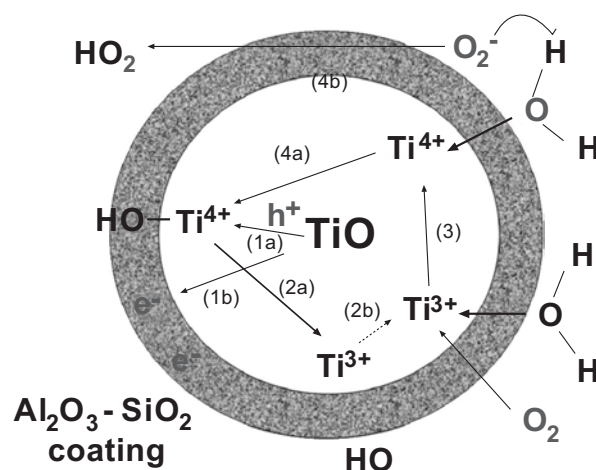


Fig. (4). Surface photocatalytic activity of Titanium Dioxide.

In the initiation step free radicals are generated. During photooxidation these radicals are formed due to a photolysis reaction of one of the chromophores present. The propagation reactions are thermal reactions and these have been studied in more detail. The rate of the reaction of oxygen with alkyl radicals is very high and that is why the rate of the propagation is largely determined by the ease of hydrogen atom abstraction in the second step of the propagation. The propagation reaction is a repeating reaction; photochemically, hydroperoxides can decompose homolytically into alkoxy and hydroxy radicals which can initiate another propagation cycle [17-19]. Carbonylic products such as ketones are produced as a result causing in chain scission reactions reducing the polymer molecular weight and sometimes

inducing crosslinking reactions with property losses. Termination reactions are bimolecular. In the presence of sufficient air, which is normally the case for the long-term degradation of polymers, only the reaction of two peroxy radicals has to be considered. Here the reaction depends on the type of peroxy radical present. Aside from these processes polyaromatics and heterochain polymers exhibit further complex reactions but for the purposes of this article the main processes of concern are those induced by the catalytic effect of the titanium dioxide. The ability of pigments to catalyse the photooxidation of polymer systems has also received significant attention in terms of their mechanistic behaviour. In this regard much of the information originates from work carried out on TiO₂ pigments in both polymers and model systems [20-27]. To date there are three current mechanisms of the photosensitised oxidation of polymers by TiO₂ and for that matter other white pigments such as ZnO. All three schemes are illustrated in Fig. (4). These are:

1. The formation of an oxygen radical anion by electron transfer from photoexcited TiO₂ to molecular oxygen [20]. A recent modification of this scheme involves a process of ion-annihilation to form singlet oxygen which then attacks any unsaturation in the polymer [28].
2. Formation of reactive hydroxyl radicals by electron transfer from water catalysed by photoexcited TiO₂ [29]. The Ti³⁺ ions are reoxidised back to Ti⁴⁺ ions to start the cycle over again.
3. Irradiation of TiO₂ creates an exciton (p) which reacts with the surface hydroxyl groups to form a hydroxyl radical [20]. Oxygen anions are also produced which are adsorbed on the surface of the pigment particle. They produce active perhydroxyl radicals.

During the weathering of commercial polymers containing white pigments such as titania oxidation occurs at the surface layers of the material which eventually erodes away, leaving the pigment particles exposed. This phenomenon is commonly referred to as "chalking" and has been confirmed by scanning electron microscopy. Methods of assessing pigment photoactivities have attracted much interest from both a scientific and technological point-of-view. Artificial and natural weathering studies are tedious and very time consuming. Consequently numerous model systems have been developed to rapidly assess their photochemical activities. Most of these systems undergo photocatalytic reactions to give products which are easily determined, usually by UV absorption spectroscopy, HPLC or GC and microwave spectroscopy etc.

PHOTOACTIVITY TESTS FOR 2-PROPANOL OXIDATION AND HYDROXYL CONTENT

These are specific tests to ascertain titanium dioxide photoactivity. The various types and grades of titania discussed in this chapter are listed in Table 2. The oxidation of 2-propanol to yield acetone is a specific methodology and this has been related to oxygen consumption during irradiation of the medium in the presence of the titania particles [30]. The hydroxyl content relates to the concentration of hydroxyl functionalities present on the pigment particles and is often related to activity [31]. The data for both tests are compared in Fig. (5).

There are a number of correlations and trends within the data. Firstly, all the nano-particle grades exhibit higher photoactivities than the pigmentary grades. Thus, for oxygen consumption the anatase A is more active than the rutile types B and D, the latter being the least active and most durable pigment. Secondly, of the nano-particles the rutile

Table 2. Properties of Pigmentary and Nano-Particulate Titanias

Sample	BET Surface Area m ² /g	Particle Size	Surface Treatment	% Surface Treatments
A-Anatase Normal	10.1	0.24 nm	None	
B-Rutile Normal	6.5	0.28nm	Al	1
C-Rutile Normal	12.5	0.25 nm	Al	2.8
D-Rutile Normal	12.5	0.29 nm	Al	3.4
E-Nano Anatase	44.4	20-30 nm	None	
F-Nano Anatase	77.9	15-25 nm	None	
G-Nano Anatase	329.1	5-10 nm	None	
H-Nano Anatase	52.1	70 nm	Hydroxy Apatite	5
I-Nano Rutile	140.9	25 nm	None	
J-Nano Rutile	73.0	40 nm	Al,Zr	13
K-Nano Anatase	190.0	6-10 nm	Al,Si,P	20
L-Nano Rutile	73.0	30-50 nm	Al,Zr	13
M-Nano Anatase	239.0	71nm	Al,Si,P	12
N-Nano Anatase	190.0	92 nm	Al,Si,P	20
O-Rutile Normal	12.5	250 nm	Al,Si,P	3.5

grade I is the most active in both tests. The three anatase grades E, F and G exhibit increasing activity with hydroxyl content while for oxygen consumption F is the greater. It is nevertheless clear from the data that nanoparticulates are significantly more active.

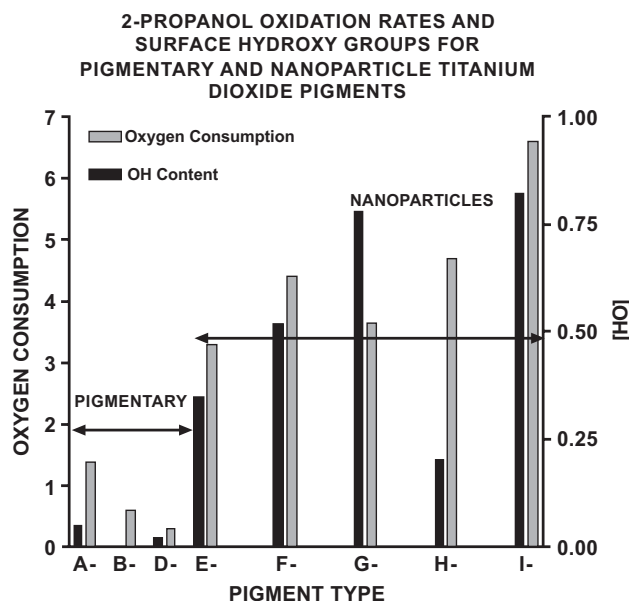


Fig. (5). Comparison of hydroxyl content and oxygen consumption rates for 2-propanol oxidation with pigmentary and nano particle titanium dioxide.

ENVIRONMENTAL BENEFITS

Environmental issues play an important role in the applications of titania fillers. These include the use of their photocatalytic behaviour in the development of self cleaning surfaces for buildings i.e. antisoiling and antifungal growth and VOC/NO_x reduction (emissions). The latter can cause lung damage by lowering resistance to diseases such as influenza and pneumonia while in combination with VOC's it produces smog and contributes to acid rain causing damage to buildings. From a commercial point-of-view such benefits have enormous implications. Japanese scientists [32] have been actively exploiting the development of a variety of materials and a number of European ventures have followed suit, most notably in Italy with Global engineering and Millennium Chemicals as examples and the European funded PICADA Consortium [33]. Here, developments range from self-cleaning and de-polluting surfaces and facades based on nano-titania activated coatings and cementitious materials. These applications include, anti-soiling, de-pollution of VOC's and NO_x contaminants and anti-fungal/microbial activities. Numerous reports have appeared in newspapers and magazine articles highlighting such applications i.e. self-cleaning paving and building blocks and facades that can also de-pollute the surrounding atmosphere. Internal coatings and paints for sanitisation and elimination of MRSA as well as for example, clothes and textiles that supposedly never need cleaning (although in many cases this is undoubtedly an exaggeration and was for public awareness of the potential). The cements are normally loaded up to 3% w/w for optimum activation and cost-efficiency.

SELF CLEANING EFFECTS: PAINTS/SOL-GEL COATED MATERIALS

The relative photoactivities of the nanoparticles and pigments may be compared by measuring their influence in the first instance, on the durability for example, of an 18% w/w PVC based alkyd paint matrix. Mass loss and gloss loss are the two industrial parameters often used and the latter is compared in Fig. (6) for the range of pigments and nanoparticles given here. These results clearly show that photoactivity is divided into two main trends. For gloss loss all four nano-particle anatase pigments are the most photoactive. The rutile pigments B and D and the anatase pigment A exhibit similar activity to that of the nano-particle rutile grade I.

Thus, in terms of self cleaning this can be described in a number of formats. For coatings and cementitious coated materials this would imply a surface which under light activation would have the ability to continuously destroy or "burn-off" by oxidation the surface dirt layers whether they be, carbonaceous, oil or soil. This can be seen visually in some of the commercial trials undertaken by Millennium Chemicals in tunnels in Italy (in conjunction with Global Engineering, Milano). The photocatalytic activity of eco-coatings can be measured by for example, determining the fading rate of an impregnated dye such as Methylene Blue. This is illustrated in Fig. (7) where over a given period of light exposure a siloxane coating with photocatalysts exhibits a rapid dye fade compared with the un-doped coating with the PC105 grade exhibiting the greatest activity. In reality this is further illustrated by the photographs of real trials in Milan shown in Fig. (8) where the photocatalytic cement remains clean after a period of use compared to that for un-doped cement.

For paints and coatings the idea is actually to limit the oxidation and chalking of the paint film to the very near surface layers such that over time with weathering rain water will wash the top layer leaving an underlying clean fresh surface. The other like the cementitious materials the surface deposits are oxidised or "burnt-off" leaving the surface layer clean. In the former case it is important that the coating exhibits high durability for a reasonable cost-effective stable system. Also, the paints chosen must be stable to flocculation and viscosity changes, cure or dry at ambient temperature and ideally be water based to avoid further environmental problems. Most polymers are carbon based and are unlikely to be photo-resistant but water based acrylic latex and polysiloxane paints have been evaluated. In the first instance four types of acrylic water based paints were evaluated in terms of relative stability toward photoactive nanoparticles. Here a special sol-gel grade of anatase was prepared in the laboratory with no post firing. Particles of varying sizes were also prepared *via* this route. The relative paint stabilities with and without the anatase sol particles (10-20 nm) at 5% w/w are shown in Table 3 after 567 hours of weathering. Of these paint formulations only the Polysiloxane BS45 (Wacker) proved to be resistant to the photocatalytic effects of the titania particles. The styrene-acrylic, poly(vinyl acetate) and acrylic copolymers all showed high degrees of chalking (weight loss).

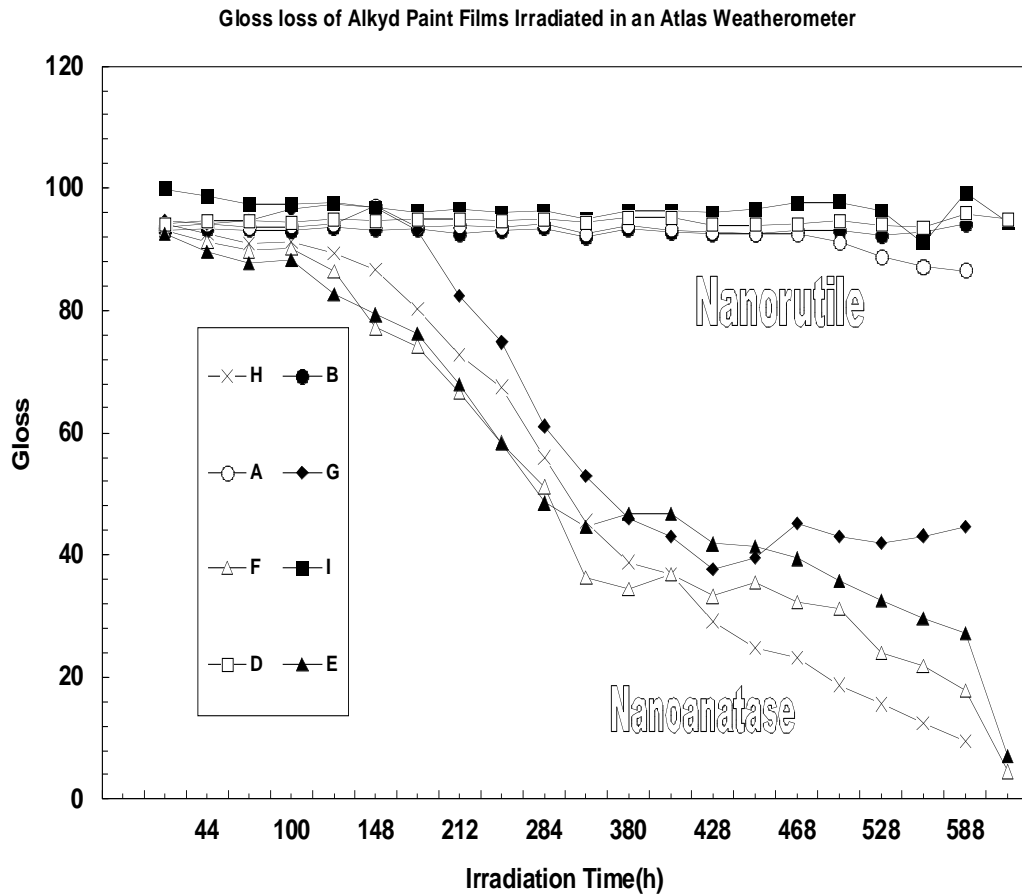


Fig. (6). Loss of gloss during weathering of an alkyd Paint film in an Atlas weatherometer.

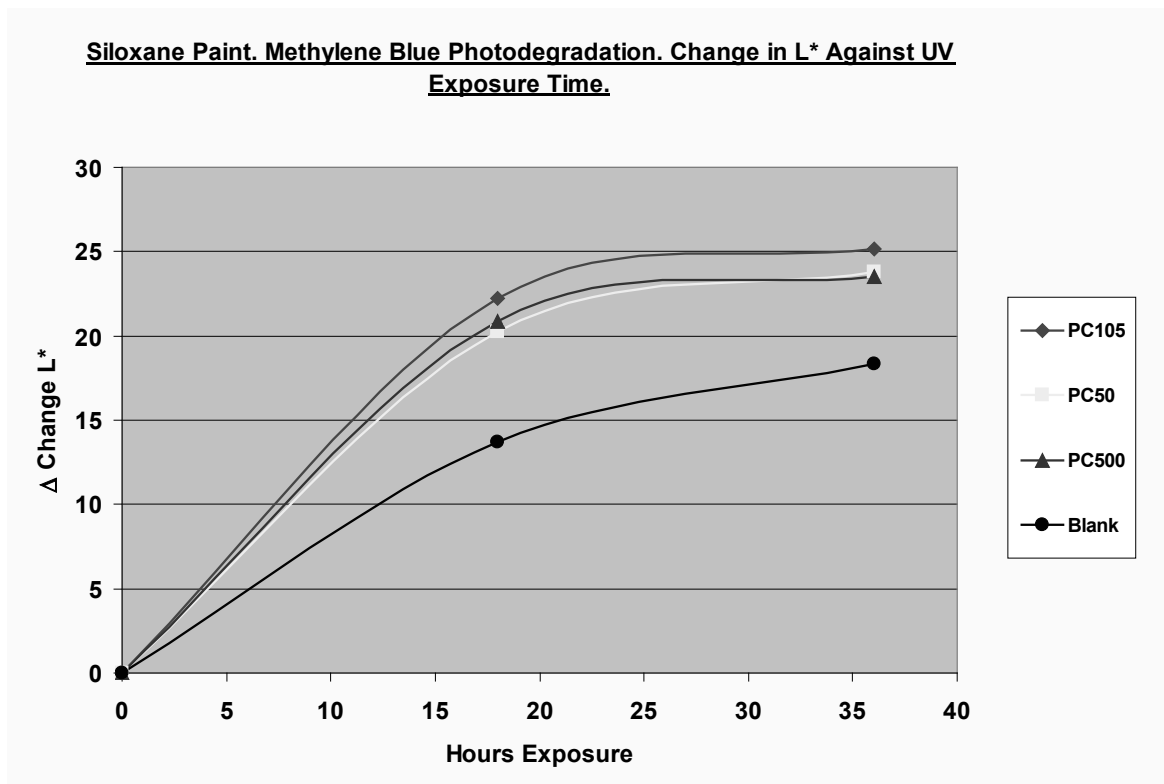


Fig. (7). Fading rate of Methylene blue dye impregnated into a siloxane paint with and without different nano-Titania photocatalysts.

Milano, Ecotunnel in Via Porpora

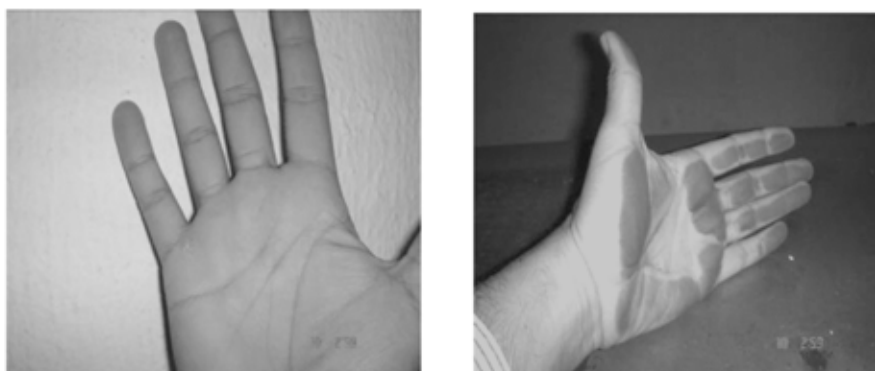


Fig. (8). Cementitious materials with and without photocatalyst coating in a Motorway Tunnel in Italy after 3 months exposure.

Table 3. % Weight Lost After 567 Hours Atlas Exposure Various Polymers Plus 5% Anatase sol. 10-20 nm

Details	% Wt. Loss
Styrene Acrylic	12.2
Styrene Acrylic + Anatase sol.	97.3
PVA copolymer	11.4
PVA copolymer + Anatase sol.	97.9
Acrylic copolymer	7.4
Acrylic copolymer + Anatase sol.	101.0
Polysiloxane BS45	23.3
Polysiloxane BS45 + Anatase sol.	13.6

Aside from organic based paints there are a number of inorganic paints in the market place a number made from complex alkali metal silicates. Because of their inorganic nature they tend to be significantly light stable. An example of the self cleaning effect of a typical silicate based paint is demonstrated by the fading data on methylene blue dye in Fig. (9). It is seen that photobleaching of the dye occurs more rapidly in film with photocatalyst than an un-dyed (un-doped) film and that this increases with increasing concentration of PC-105 nanoparticles.

Another method used to potentially enhance durability of a substrate whilst simultaneously controlling photocatalytic activity is to dope the paints with mixtures of durable and catalytically active grades of titanium dioxide. In this regard mixtures of pigmentary rutile O and nanoparticle anatase F pigments appear to provide one interesting illustration option

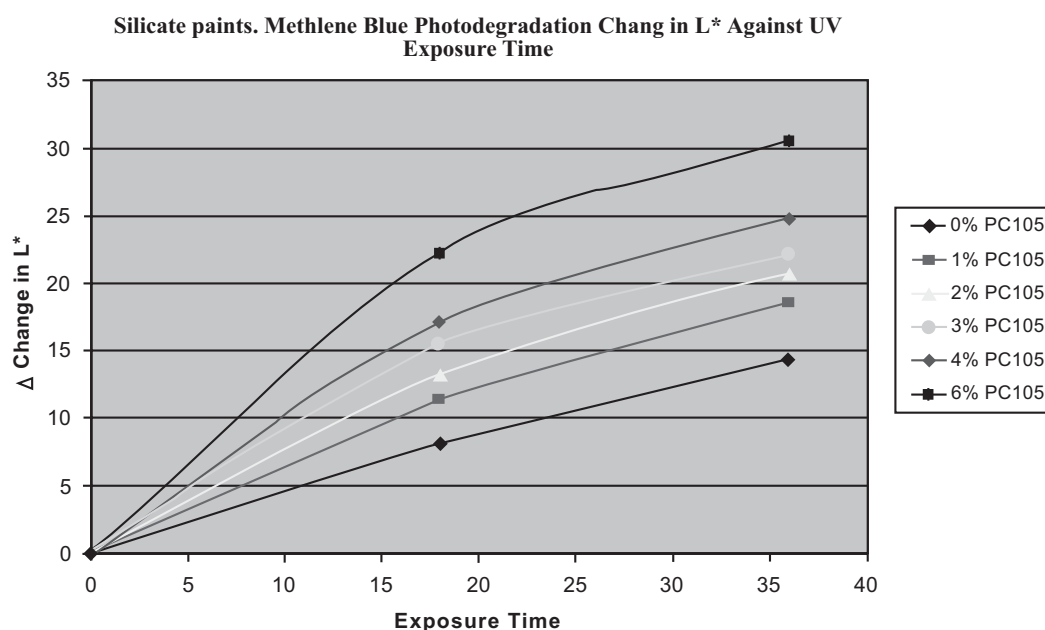


Fig. (9). Change in colour difference factor L with exposure time for methylene blue impregnated silicate paint films with increasing nanoparticle titanium dioxide PC-105.

with the former inducing some level of base stability while the presence of the latter gives rise to surface activity. Figs. (10) and (11) illustrate this effect for a siliconised polyester coating exposed in a QUV weatherometer for gloss and mass loss respectively. Gloss loss is seen to be gradually reduced with time the effect increasing with increasing loading of anatase nanoparticle F. Mass loss is also seen to increase gradually with increasing levels of the same nanoparticle. In this case it is evident that only low levels of shedding/chalking occur with time such that the paint film retains some level of durability except for the very near surface layer. A similar but perhaps more extreme effect is shown in

Table 2 for a Lumiflon fluorinated acrylic paint film. At 10 and 20% concentrations of the nanoparticles G, F, E and H chalking is quite high while the pigmentary rutile O at 20% w/w only gives a 4.7 mass loss value. The pigmentary uncoated anatase A is also an option giving high levels of chalking at 10 and 20% w/w. Thus, control of pigment type and particle size as well as their concentrations is a critical area of development for effective self cleanable paint surfaces, the effect varying also with the paint formulation. In this regard coatings could effectively be developed to suit a particular type of environment.

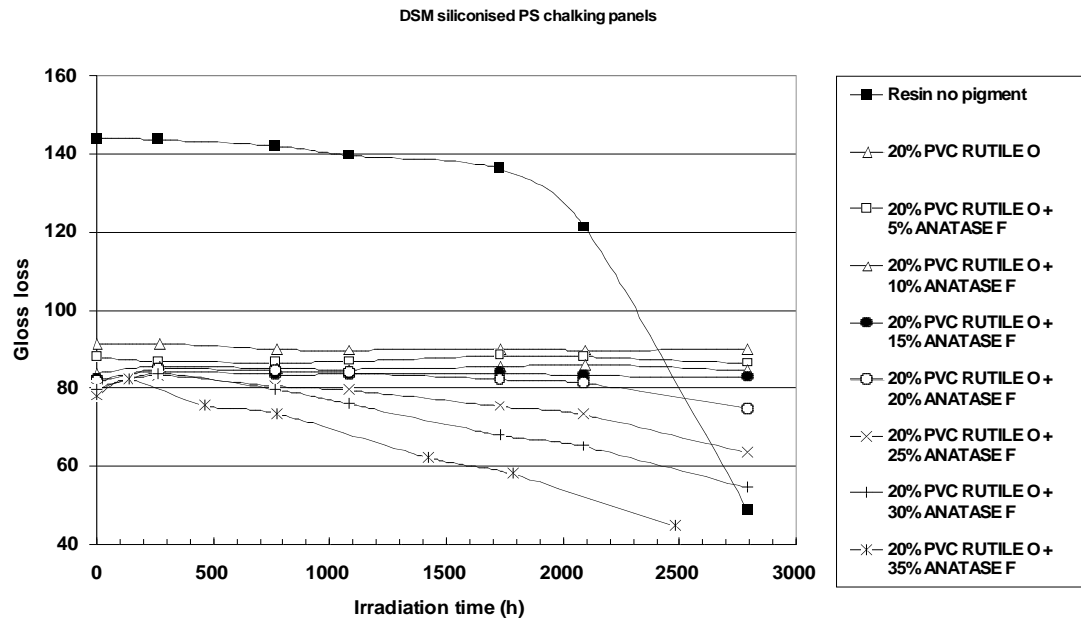


Fig. (10). Gloss loss versus irradiation time in a QUV weatherometer for a DSM siliconised polyester resin with 20% w/w Rutile pigment O plus increasing levels of 5, 10, 15, 20, 25, 30 and 35 % w/w of nanoparticle anatase F.

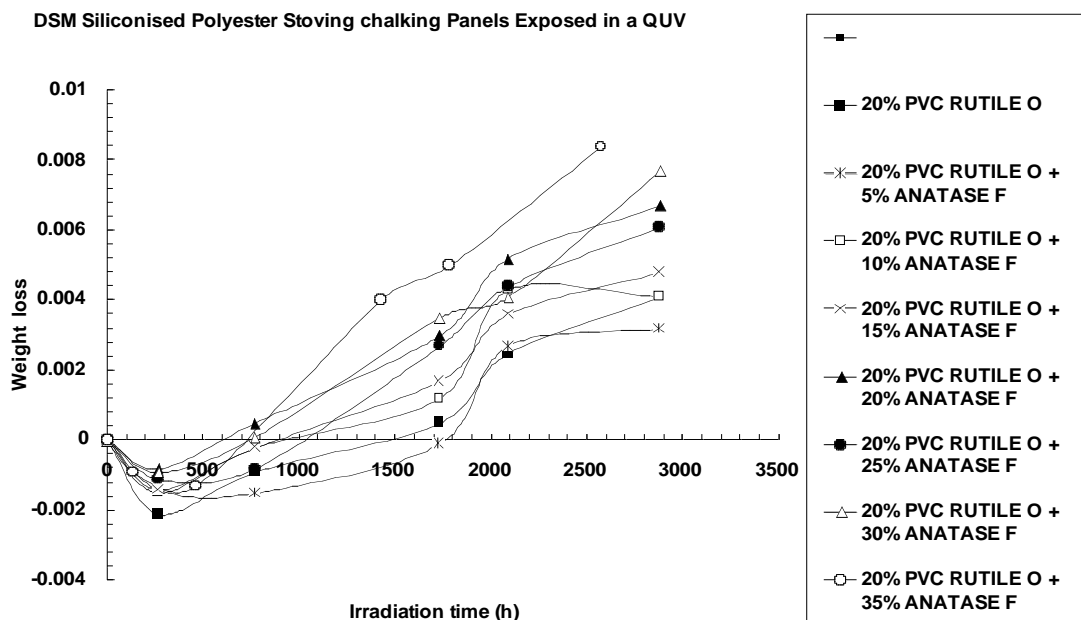


Fig. (11). Mass loss versus irradiation time in a QUV weatherometer for a DSM siliconised polyester resin with 20% w/w Rutile pigment O plus increasing levels of 5, 10, 15, 20, 25, 30 and 35 % w/w of nanoparticle anatase F.

Table 4. Lumiflon Paint Pgmented with RCL-696/Nano Titanium 546 Hours Atlas Exposure

Nano Titanium Dioxide	Pigmentary TiO ₂	Weight Loss
10% wt PC500	RCL-696	19.0
20% wt PC500	RCL-696	66.5
10% wt PC105	RCL-696	31.0
20% wt PC105	RCL-696	62.8
10% wt PC50	RCL-696	30.4
20% wt PC50	RCL-696	39.0
10% wt Showa Denko	RCL-696	77.0
20% wt Showa Denko	RCL-696	105.4
10% wt AT1	RCL-696	16.6
20% wt AT1	RCL-696	43.2
20% wt PC500	None	97.6
20% wt PC105	None	128.7
20% wt PC50	None	121.4
20% wt Showa Denko	None	146.8
20 wt AT1	None	138.7
None	RCL-696	4.7
Clear resin blank	None	5.4

From a comparative point-of-view the weatherability in a QUV of a silicate inorganic and a vinyl paint are shown in Fig. (12). The vinyl paint is clearly more unstable with the

effects of the PC105 nano-titania increasing weight loss with increasing concentration.

ANTI-BACTERIAL EFFECT

The ability of the nanoparticles to destroy bacteria and funghi has also been actively pursued and some data from our laboratories is demonstrated here. The type of photocatalytic medium, nanoparticle and bacteria/funghi all play an intimate key role in performance. There are a number of tests one can apply [34-36] the simplest evaluation being the typical zone of inhibition on agar plates where the growth of bacteria are measured around a paint film. Staphylococcus growth is shown on agar plates in Fig. (13) for typical silicate paint films with and without PC 105 nanoparticles. On the right hand picture plate a clear zone of inhibition is seen to develop compared with that for the un-doped film.

Similar tests have also been undertaken in our laboratories on the titanium dioxide powders. AureusHere *E. coli* were used where their destruction (measured in terms of colony forming units) after irradiating with UV light in the presence of the titania particles is plotted against irradiation time. A study on the range of titania powders showed that there was (Fig. 14) an inverse relationship between antibacterial activity and particle size: for the pigment powders, Pigment E>H>F>G=A, with a sol-gel colloid dispersion C and Degusa P25 having the greatest effects. However, the experimental conditions used did provide some confounding factors which required clarification in order to identify the best experimental method, and the most effective pigments in terms of antibacterial activity as mentioned previously. Here the particles were dispersed in a Calgon media and this evidently reduced activity on the plate.

Weight loss evolution for vynil paint and pigment PC105 on exposure in QUV relative weight loss

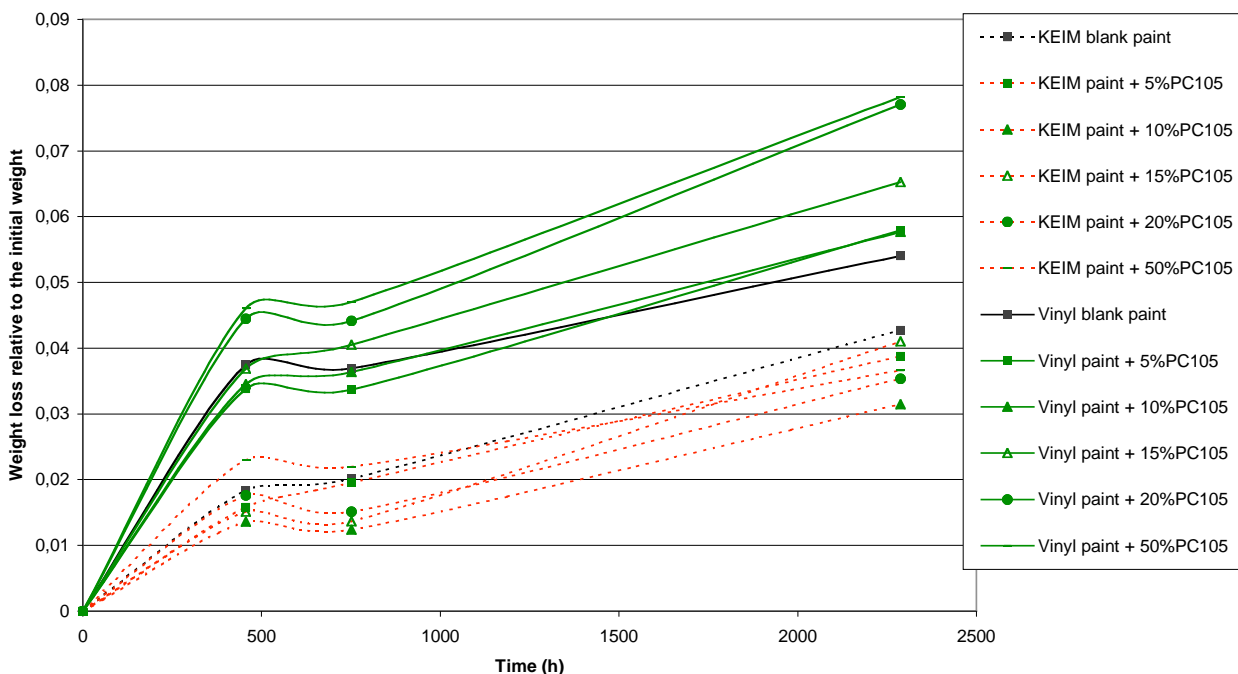


Fig. (12). Weight loss comparison for a silicate inorganic (Keim, Shropshire, UK) and standard acrylic vinyl paint with increasing levels of nano-titania PC105.

EXAMPLE OF TEST (Bacterial inoculum)

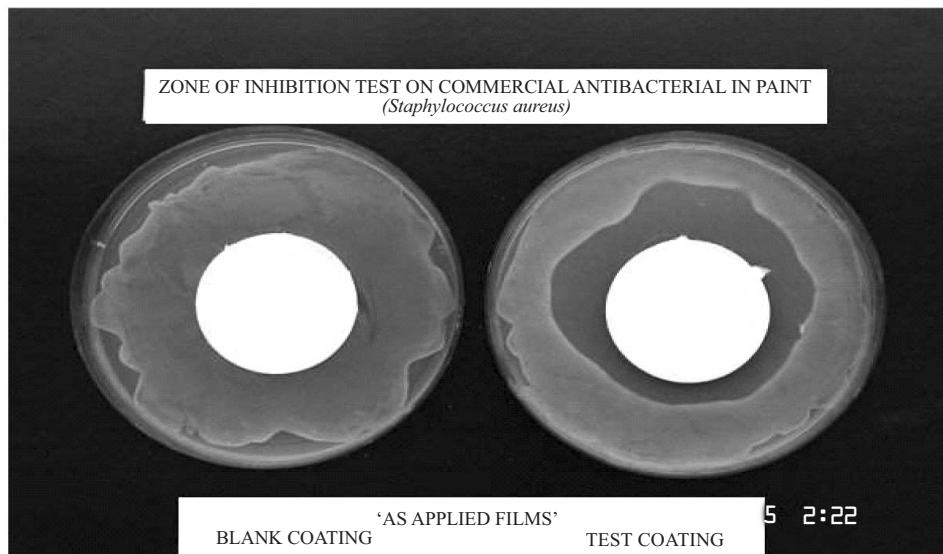


Fig. (13). A typical anti-bacterial evaluation on an agar plate medium for eco-paint films with and without nanoparticulate photocatalyst titania.

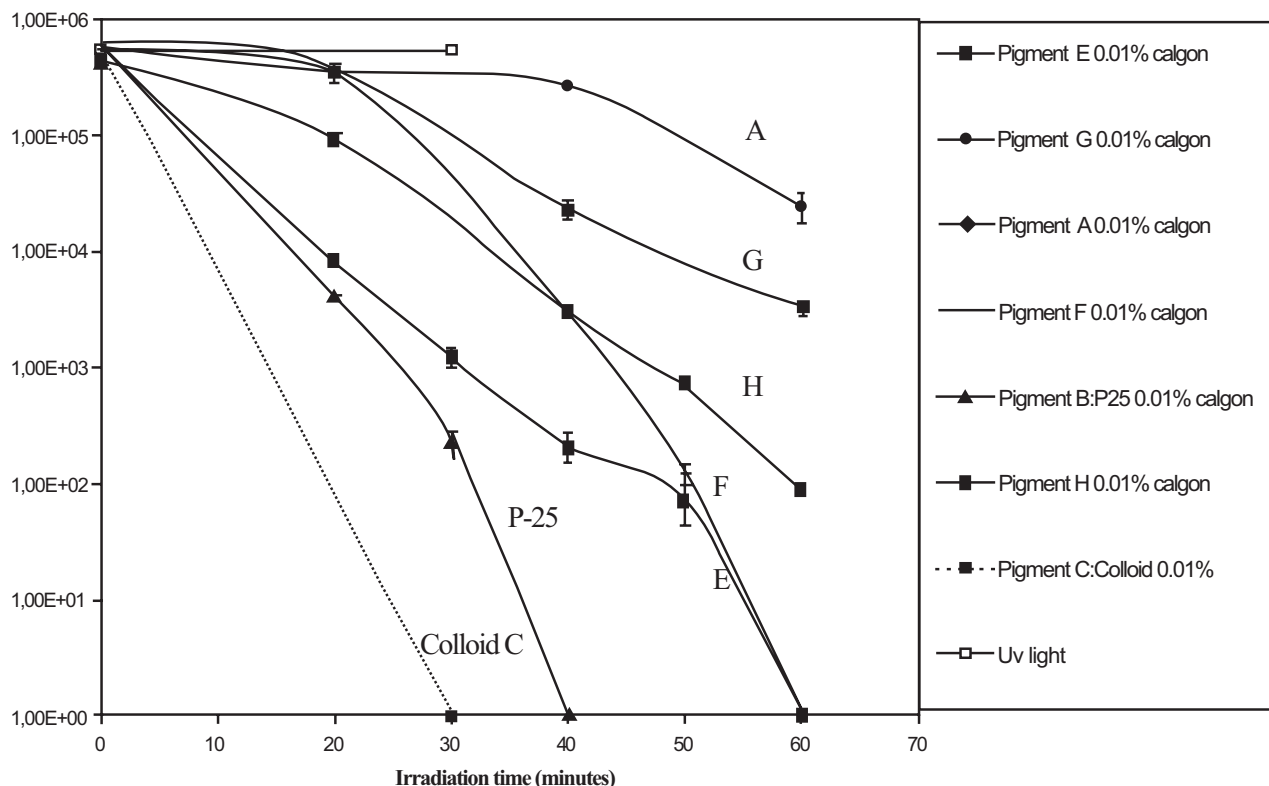


Fig. (14). Photocatalytic bactericidal effect of pigments A, B, E, F, G, H powders and C (colloid) at 0.01% in stirred conditions, unwashed cell suspensions.

In general, the antimicrobial effect increased with increasing concentration of nanoparticles (Fig. 15) up to 0.04%. In the absence of a nan dispersion effect the activity of the nanoparticle E was comparable to that of the Degusa P25, followed by F and G and with little difference between A, H and D and the mercury lamp control (Fig. 16). Similar

results were observed at 0.02% in our work. For the nanoparticles E, F, G, a further enhanced effect was noted at 0.1%, but the effect of P25 was reduced.

The enhanced activity of C over its derivative pigment G was lost when C was dried and ground (Fig. 17). This find-

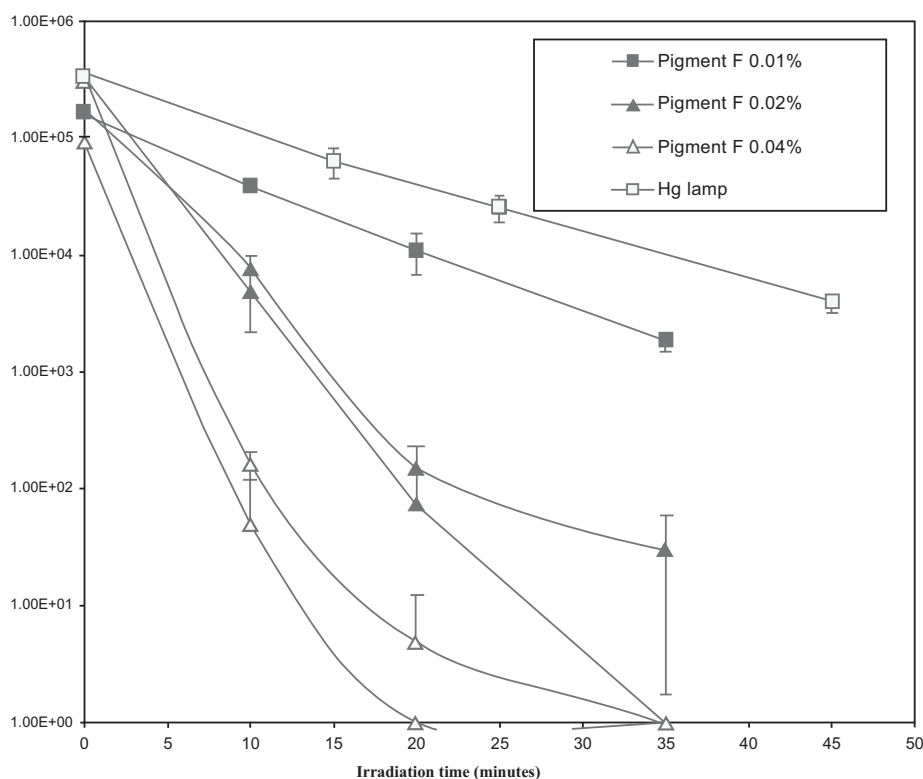


Fig. (15). Effect of concentration of pigment F on photocatalytic bactericidal effect.

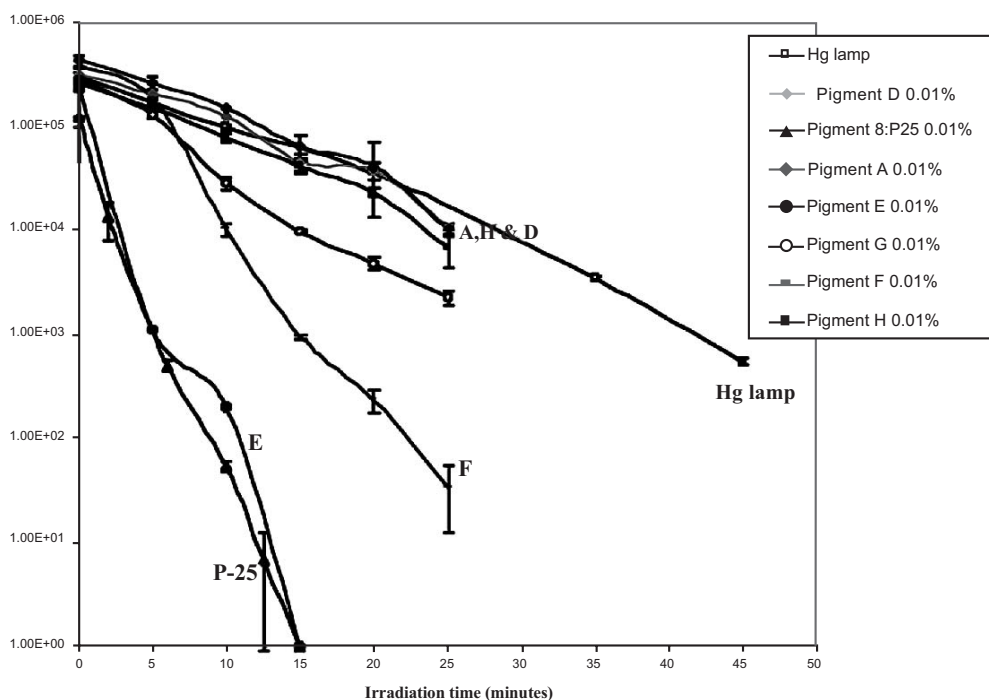


Fig. (16). Photocatalytic bactericidal effect of pigments A, B, D, E, F, G, H at 0.01%, using washed cell suspensions.

ing demonstrates that the drying process has a marked effect on activity, due to a decrease in surface area during aggregation, and to a decrease in dispersion stability in water.

Pigment E has the most reactive surface because it has fewer defects, which increases the efficiency of the photo-generated radicals from our microwave analysis [33]. Thus

pigments calcined at higher temperatures (E>F>G) have better crystallinity and therefore higher antibacterial activities.

The UV light itself has little effect on the bacteria while the pigmentary grade of anatase A has a small effect while the nanoparticle G has a somewhat greater effect. However, the most interesting feature of this data is the very high de-

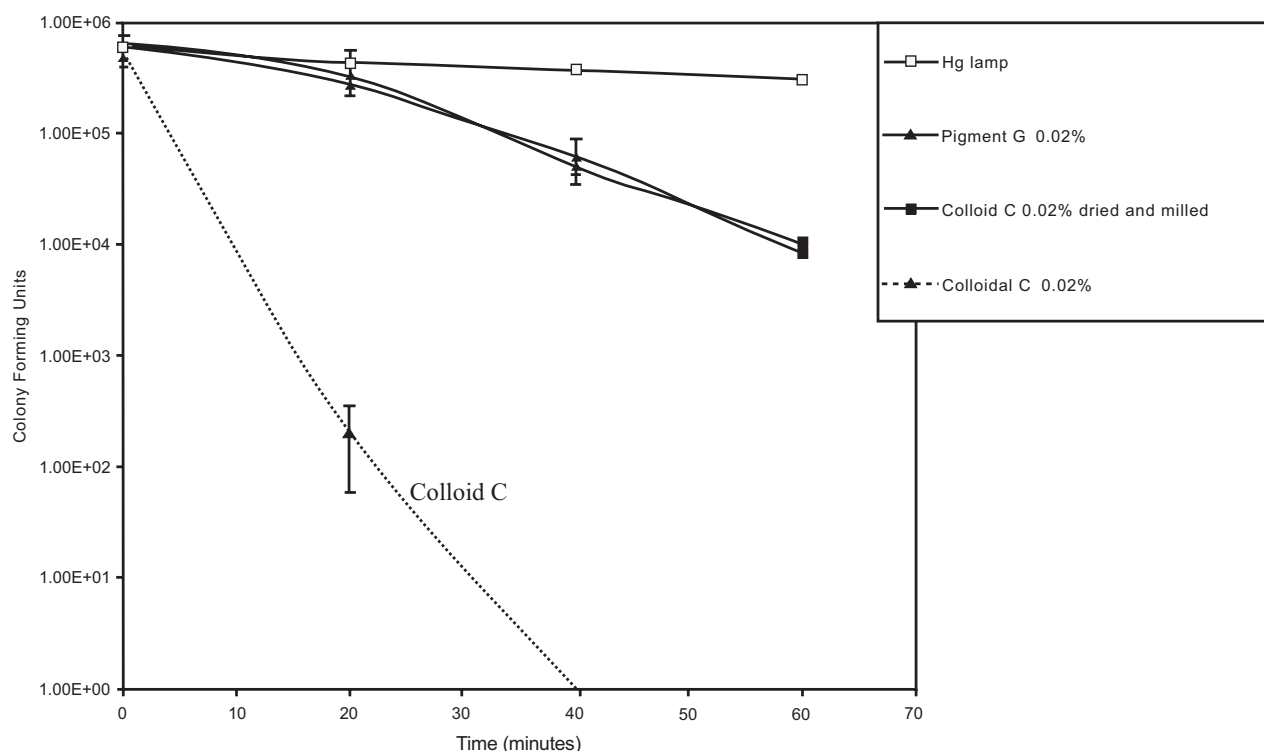


Fig. (17). Photocatalytic bactericidal effect for C colloid suspension, C dried and milled, and pigment G powder (unstirred).

structive effect of the mixed phase nanoparticle grade made by Degussa (P-25). This nanoparticle grade of titania is well established in the literature in terms of its high photoactivity [32]. In this work a grade of nanoparticle anatase G was prepared in the laboratory whereby the particles were seeded from solution and then dried but not subsequently oven fired. This so-called washed form of titania is seen in the data to be higher in activity than that of the Degussa material. This effect is currently being investigated further in terms of hydroxyl content and hydrogen peroxide generation.

The overall effect of activity will depend on whether more TiO_2 is activated as a consequence of increased surface area, or whether less TiO_2 is activated because less light passes through the suspension due to light scattering. Larger aggregates of particles sediment in a liquid system, and an increased concentration of pigments shows less of an antimicrobial effect since less light passes through the suspension if the cell-particle mixture is not stirred. Conversely, Calgon milled pigments which are nanometer sized also scatter light significantly at high concentrations and decrease activity (optimum loading 0.01%), thus the optimum activity is presented by nanoparticle powder aggregates in this work. The most important aspect to consider in terms of antibacterial inactivation is the relative sizes of the titanium particles/aggregates and the bacterial cell. *E. coli* measures approximately $1 \times 3 \mu\text{m}$; a benzene molecule is $0.00043 \mu\text{m}$. Porosity of the pigment has no bearing on the antimicrobial effect, whilst the chemical pollutant can diffuse into the porous particle structure. Thus, the higher surface area of pigment G did not enhance any antibacterial effect. It has been verified by disc centrifuge in our study that the three nanoparticulate powder pigments E, F, G were aggregated into $0.7 \mu\text{m}$ particles. In this case, they would all offer com-

parable active areas to bacteria. Only the inherent ability of the pigments to generate radicals will affect antibacterial activity. Thus, the process is more sensitive to structure (crystallinity) than to texture (surface area) and follows a clear inverse relationship with particle surface area.

In addition to this data are shown the comparative effects of PC50 and PC105 with that of other nano-titanias on the destruction of *E. coli*. Like in the coating studies the PC105 is the more active while the Millennium sol-gel is the most active (finer hydrated particles). A competitive product is also shown for comparison.

In another recent experiment we examined the bactericidal effect of nanotitania (PC105, Millennium) under fluorescent light on a filter substrate. Here *E. coli* cells were tested at different TiO_2 concentrations up to 2 hours of irradiance (Fig. 19).

For the qualitative experiment, filters of low dose of TiO_2 $< 0.08 \text{ g/L}$ shows much more effective inactivation of the bacteria than those filters with higher TiO_2 dose $> 0.12 \text{ g/L}$.

There was a significant improvement in the killing efficiency when the TiO_2 dose was lower, 0.01 to 0.08 g/L, in this case, after 2 hours of exposure, samples inactivated all the bacteria. For the TiO_2 filter concentrations greater than 0.12 g/L there was a reduction of efficacy, and after 2 h there were cells remaining.

Fig. (20) shows the bacteria laid down onto the nanotitania particles in low, medium and high concentrations of agglomerates. Thus, it is expected that for uniform layers of titania particles in contact with the bacteria a higher destruction under illumination would be expected. As the monolayers build-up bacteria find places filling the holes, and so the

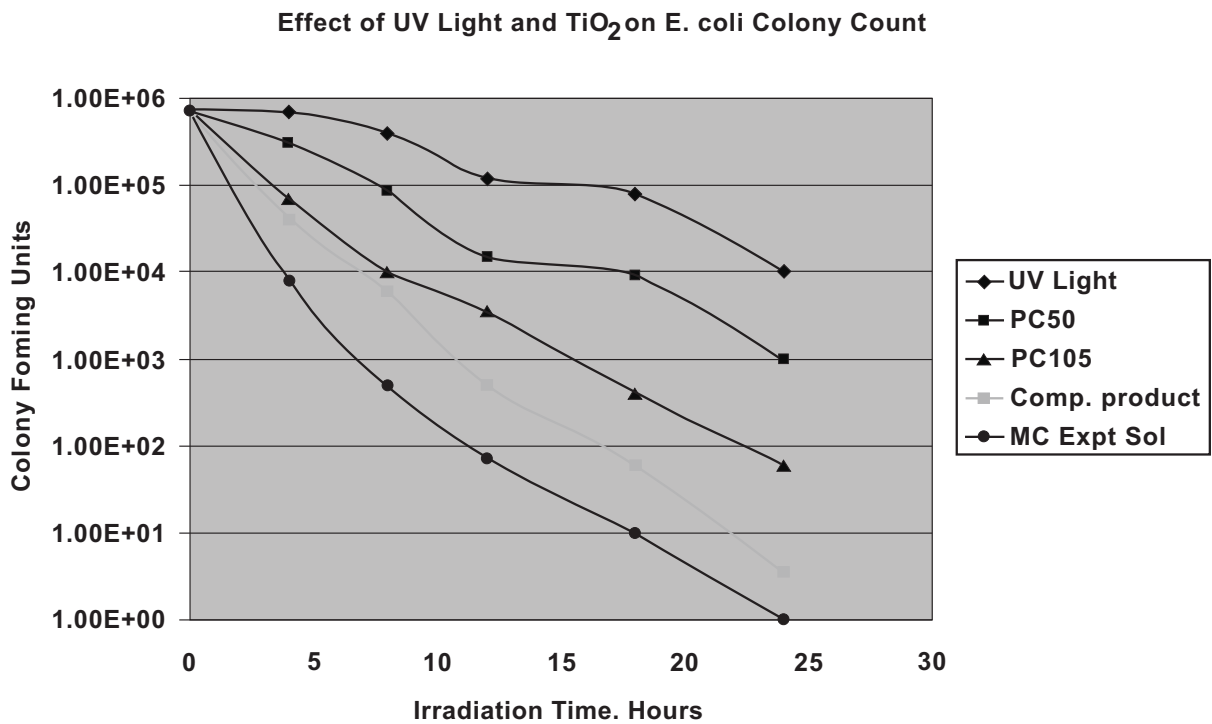


Fig. (18). Effect of UV light on the destruction of *E. coli* in the presence of different grades of Commercial and experimental Sol-Gel nanotitania products.

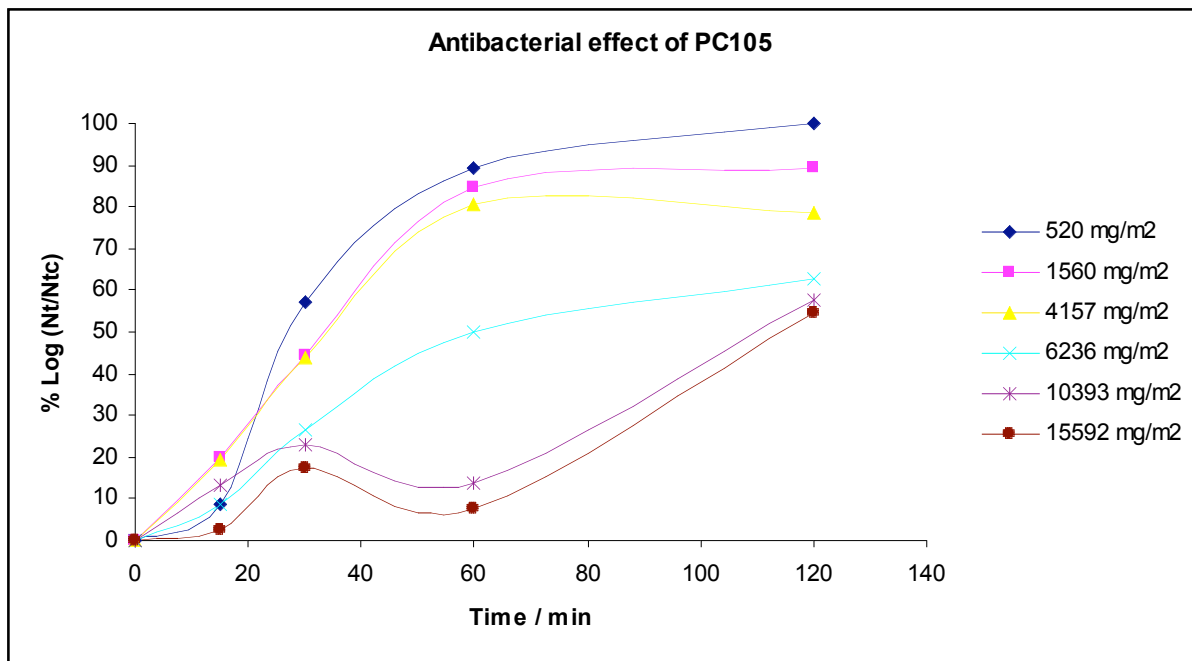


Fig. (19). Antibacterial effect of filters versus time for various concentrations of PC105 nanotitania.

Nt – is the number of CFUs (colony forming units) per mL of PC105 for *t* min.

Ntc – is the number of CFUs (colony forming units) per mL of control (PS) for *t* min.

TiO₂ can be activated easily hence the bacteria will be inactivated. As the particles build-up further beyond monolayers the bacteria can be trapped in holes where it becomes more difficult for the photons to activate the particles. Lower layers are shielded and bacteria become trapped.

Depollution: NOX /VOC Removal

The ability of photocatalytic surfaces to depollute the surrounding atmosphere with a certain radius has been well documented recently in the literature [32,33,36]. Indeed Japanese scientists have been particularly prolific in this area

for sometime now. In this part of the research work it was important to be able to develop coatings and cementitious materials with surfaces that remove NO_x , SO_2 , VOC's and potentially ozone especially in areas where such contamination is likely to be above recommended standards. Examples, would be motorway tunnels, underground car parks, busy highways chemical factories and city dwellings such as schools and airports. A pictorial representation of the key mechanistic features of the depolluting paint coatings is illustrated in Fig. (21). Here the NO_x gases are catalytically converted into nitric acid which is subsequently washed into the soil (one can argue to less environmentally harmful products and in many cases useful products in the case of plants when converted with alkalis in soils).

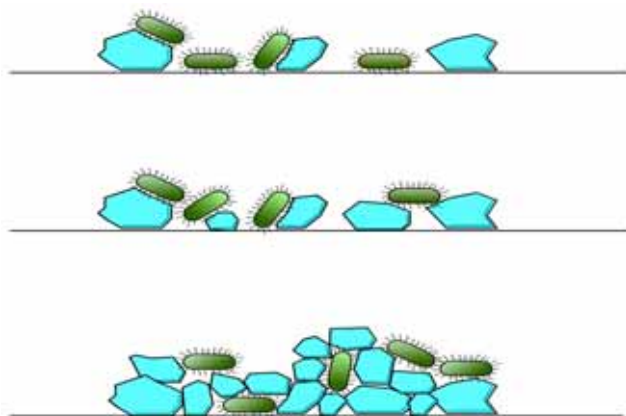


Fig. (20). Shows TiO_2 agglomerations of nanoparticles and *E. coli* in contact with the aggregates.

The materials should in this regard be durable and show little or no loss in activity with ageing as well as having the ability to inactivate nitric acid reaction products. Also, as above it should be self-cleaning. The coating may, in some cases, also need to be translucent so that existing coatings or stone work can be over-coated without any change in ap-

pearance. To some extent the coating must be photo-resistant to the effects of the nano TiO_2 and would probably need to be porous to allow contact between the TiO_2 surface and the gaseous pollutants. Nano TiO_2 is an excellent reflector of light and if the coating is porous this further increases light scattering. Some potential problems in the design of such coatings have been circumvented such as poor adhesion and poor durability in our laboratories. Also, the nitric acid formed in the reaction could damage the substrate or poison the catalytic reaction. A suitable test method was developed to measure the efficacy of the coatings studied *via* a "Signal" detection system (Fig. 22).

In this diagram shown a test film of paint is irradiated in a cell through which a standard flow rate of nitrogen is passed with a set concentration of NO_x gases. NO_x levels are measured *via* a chemiluminescence detector system before and after irradiation to give a measure of de-pollution.

Commercial dry nano TiO_2 products with a range of particle size and surface area were developed with surface areas ranging from 20 to 300 m^2/g for evaluation as indicated in Table 3. Aside from these, colloidal sol-gel particle media were also developed for easy dispersion. Even with the smallest crystallite size it is difficult to eliminate light scattering at levels above 5% at conventional coatings thickness (25 micron) due to aggregation. With special non dried sol-gel nano TiO_2 there is less light scattering because of reduced particle aggregation. It appeared that the coatings had to be porous before there was a significant activity towards gaseous reductions such as NO_x .

From the data in Figs. (23) and (24) the efficacy of NO_x removal increases significantly with both an increase in particle surface area and concentration of nanoparticle titania (anatase) in a polysiloxane paint substrate. Porosity can also be introduced by using other materials other than TiO_2 itself. Nano calcium carbonate offered the possibility of high translucency and the ability to react with nitric acid. The results

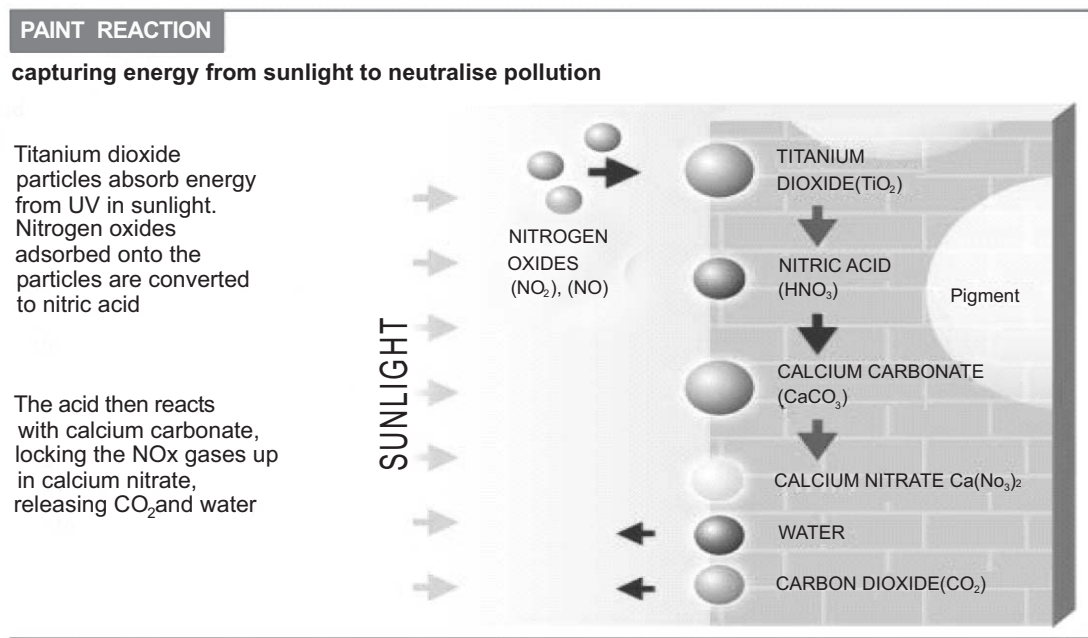


Fig. (21). Depollution scheme for photocatalytic paints and surfaces.

NOX TEST Schematic Diagram

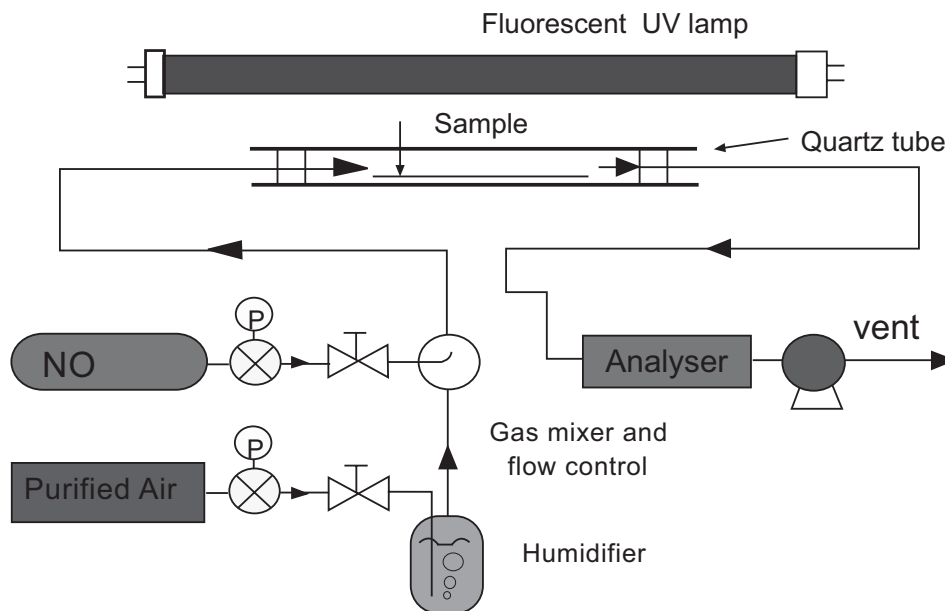


Fig. (22). Schematic diagram of NOx gas detection system for irradiated photocatalytic surfaces.

are confirmed in Fig. (23) where it is seen that not only is the NOx reduced with increasing titania doping but also with increasing levels of calcium carbonate addition.

The most interesting feature of the results however, is the influence of titania and calcium carbonate loading on the

extent of degradation of the polysiloxane paint films as measured by % weight loss. The data shown in Fig. (26) shows that in the absence of calcium carbonate the extent of degradation is low as indicated above while in its presence the rate of degradation increases with concentration from 2.5

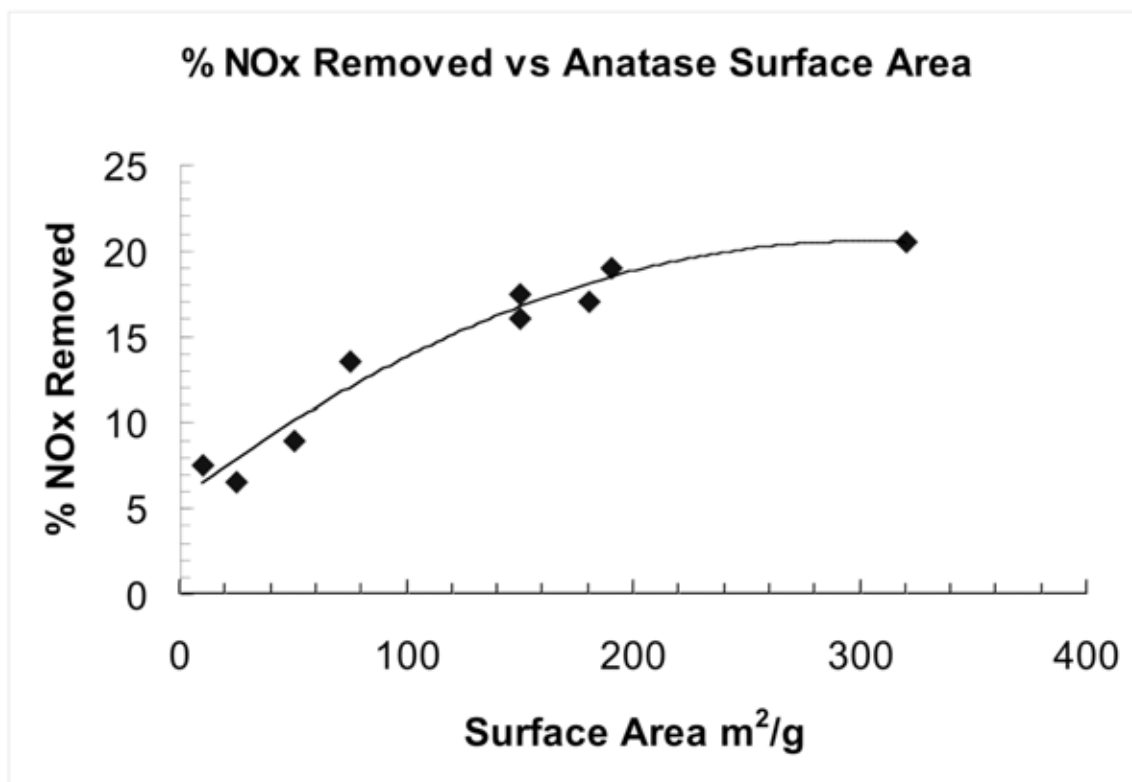


Fig. (23). Percentage concentration of NOx removed versus the surface area of anatase sol-gel particles at 5% w/w in a polysiloxane Wacker BS 45 paint system.

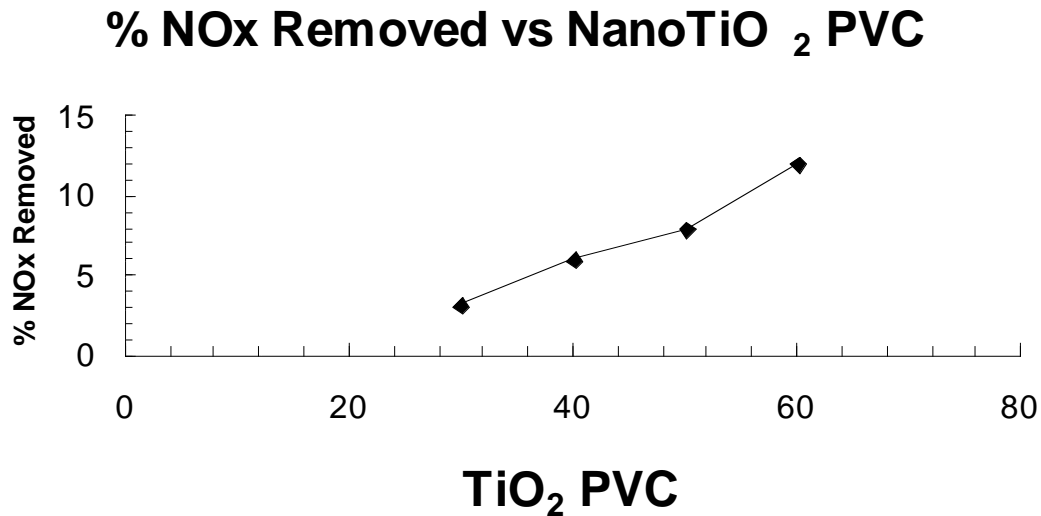


Fig. (24). Percentage concentration of NOx removed versus the concentration of anatase sol-gel particles (10-20 nm) at 5% w/w in a polysiloxane Wacker BS 45 paint system.

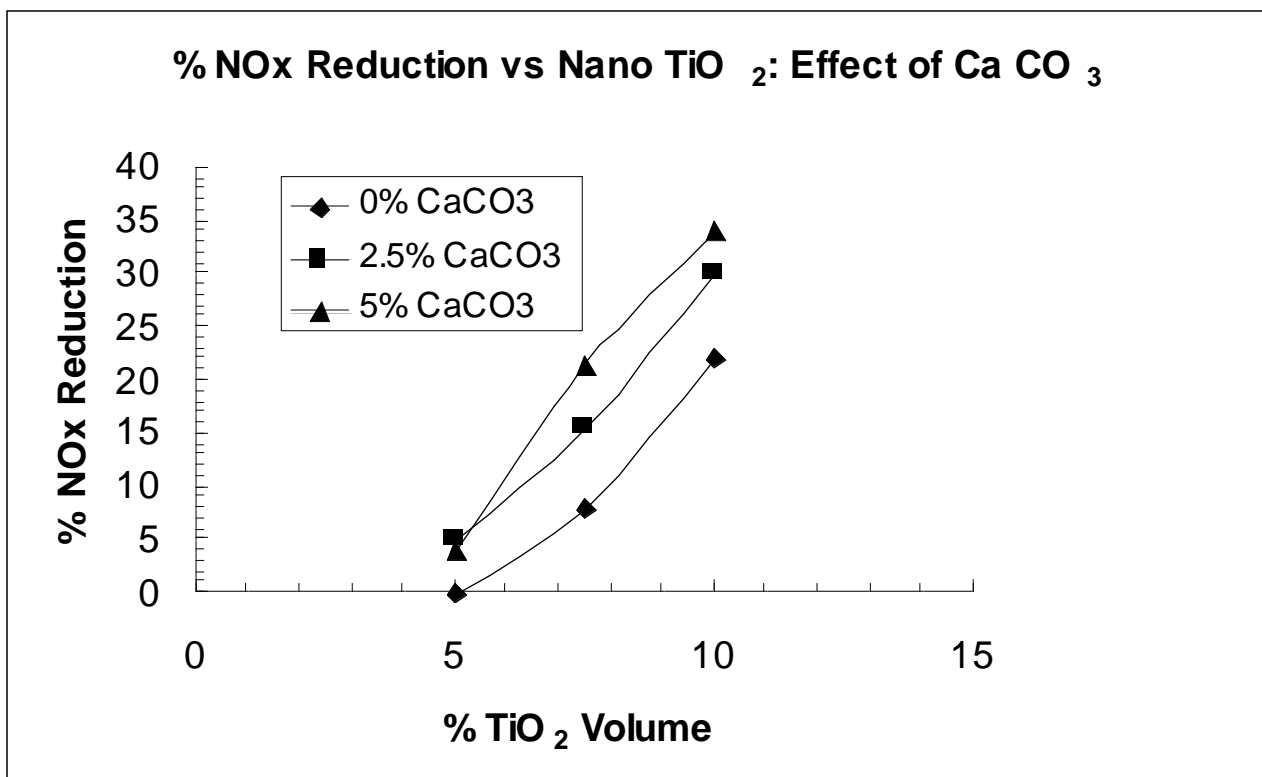


Fig. (25). Percentage NOx reduction versus volume of titania (anatase 10-20 nm) for a polysiloxane BS45 paint substrate with 0, 2.5 and 5.0% w/w of nanoparticle calcium carbonate.

to 5.0 % by weight. At 10% by weight of titania the extent of degradation is significant in the presence of the calcium carbonate. In this case the access of both moisture and oxygen through the film matrix will be enhanced. Film translucency also decreases with increasing loadings of titania and calcium carbonate particles as shown by the data in contrast ratio in Fig. (27).

Measurements on NOx reductions have also been obtained in terms of NO and NO₂ gases where it is seen that the rate of NOx destruction is clearly greater in the presence of the nanoparticles alone whilst the paint matrix gives rise to a barrier effect as might be expected (Table 5). Nevertheless, the efficacy of the paint films in destroying the NOx gases is high. The durability of a paint film in terms of NOx reduction is also important and this is illustrated by the plot in Fig. (28) for a typical Eco-silicate paint system. Here the percent-

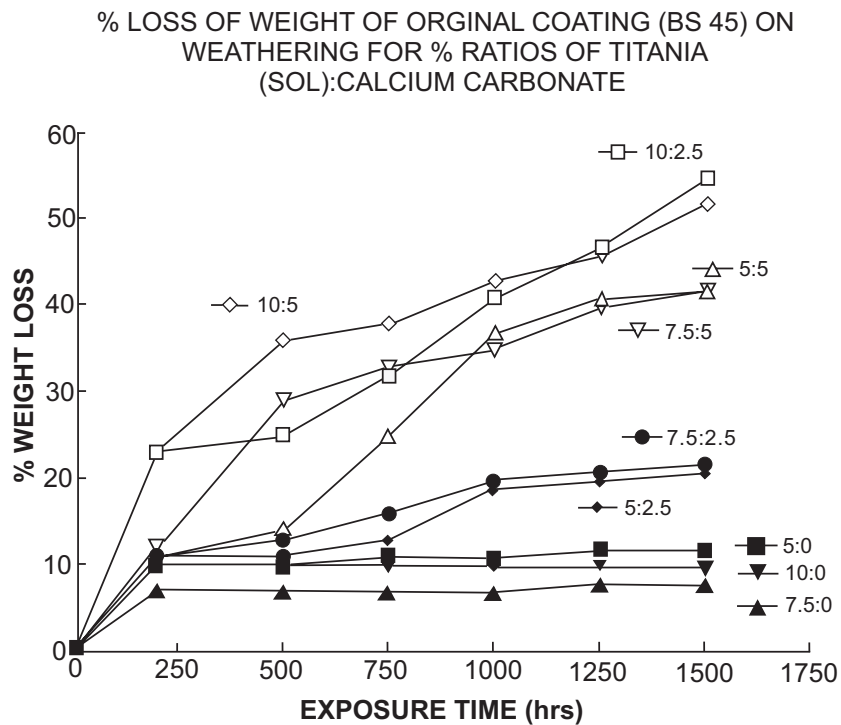


Fig. (26). Percentage weight loss versus exposure time in an Atlas Ci65 weatherometer for polysiloxane paint films (BS 45) containing different ratios of nano anatase (10-20 nm) sol-gel titania (5/7.5/10):calcium carbonate (0/2.5/10)particles.

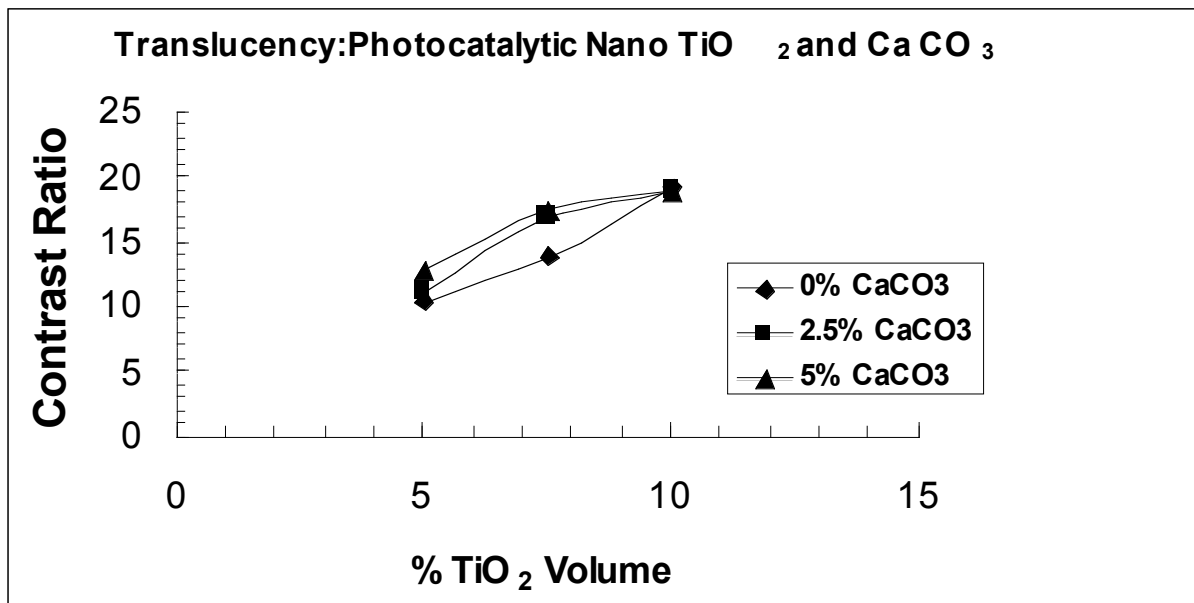


Fig. (27). Translucency (contrast ratio) for BS 45 paint films with volume addition of sol-gel anatase titania (10-20 nm) particles versus % calcium carbonate addition.

age reduction in NOx ability is reduced by only some 10% and thereafter stabilises after 12 months.

Another important factor is irradiation power or light flux density. Optimum power appears to be achieved at 0.6 mW per cm² of film as shown in Fig. (29).

The effectiveness of the Ecopaint and cementitious materials in terms of de-pollution in surrounding areas is also important and effectively demonstrated by a tunnel experiment in Fig. (30). Here one wall is effectively coated with a titania doped cement while the other is undoped. NOx meas-

urements under steady state irradiation show significantly less ppb concentrations for the titania doped left wall under both actual conditions and also *via* mathematical modelling experiments. With the same experiment using the Eco-cement coating VOC reductions can also be measured in relation to the air velocity. The data in Fig. (31) shows that as the air velocity is reduced so the VOC concentrations are effectively reduced. The benzene being unsubstituted is more difficult to photocatalytically decompose and therefore requires a slower abatement air speed for effective decomposition. The greater the degree of alkyl group substitution the

more effective and easier the decomposition rate. Alkyl groups are more easily oxidised than benzene rings.

Table 5. NO_x Reduction Comparisons for Polysiloxane Latex with and without Titania Sol-Gel and Sol-Gel Alone Using Steady-State Signal Detection Apparatus

NO _x Reduction by Percentage		
	%NO	%NO ₂
BS45 Latex	0	0
BS45 Latex + 5% Sol	84.9	9.3
Sol	84.9	55.8
Nox Reduction as µg/m ² s		
	NO µg/m ² s	NO ₂ µg/m ² s
BS45 Latex	0.000	0.000
BS45 Latex + 5% Sol	0.060	0.055
Sol	0.320	0.409

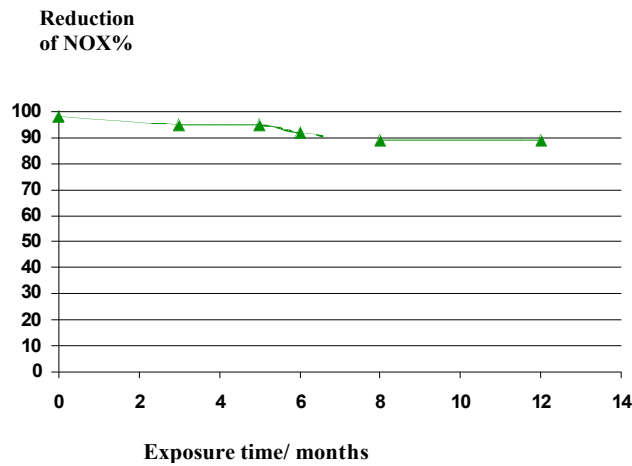


Fig. (28). Percentage efficacy of NO_x reduction for a typical silicate paint film with weathering.

Reduction of NO_x as a function of UV irradiation

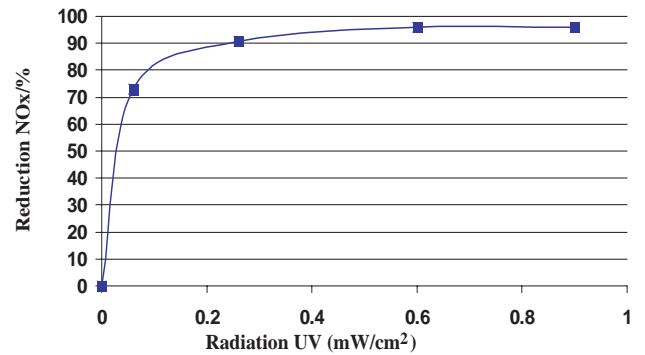
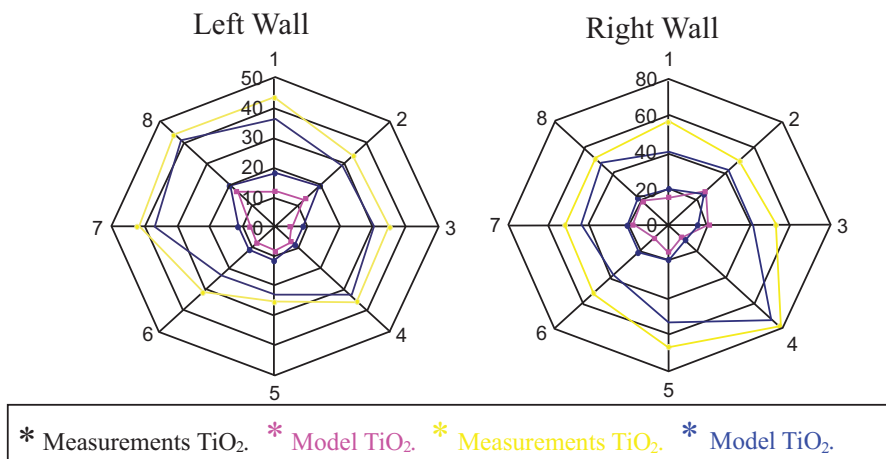


Fig. (29). Reduction in NO_x with Radiation Uv intensity for a typical Eco-silicate paint film.

EARLY COMMERCIAL PILOT STUDIES

Several commercial pilot studies have been and are still underway around locations in Continental Europe and the UK mainland on the efficacy of the coatings discussed in this article in their various formats. Some examples to highlight the success rates are presented here. If one examines the current nitrogen dioxide levels in different parts of London over a 6 year period it can be seen that they are all above the nominally acceptable limit (Fig. 32). Thus, heavy traffic congestion in one form or sort and large housing areas can all contribute to these effects. Thus, there minimisation can have subsequent health benefits to the general public as well as a cleaner more aesthetic looking environment. In one trial a School in London was treated with a photocatalytic paint system and then monitored for its efficiency in NO_x reduction through for example, the formation of nitrate levels after conversion of the NO_x. The data plots in Fig. (33) show a clear rapid build-up in nitrate levels for the photocatalytic paint areas compared to untreated areas with time of weath-

NO₂ mean concentrations (ppb) per sector with TiO₂ (Period A) and with TiO₂ (period B) for the right wall



* Measurements TiO₂ * Model TiO₂ * Measurements TiO₂ * Model TiO₂.

Fig. (30). NO_x concentrations around a tunnel wall with and without Photocatalytic Titanium dioxide doping for a cementitious facade.

Photodegradation of VOC with E-Coating

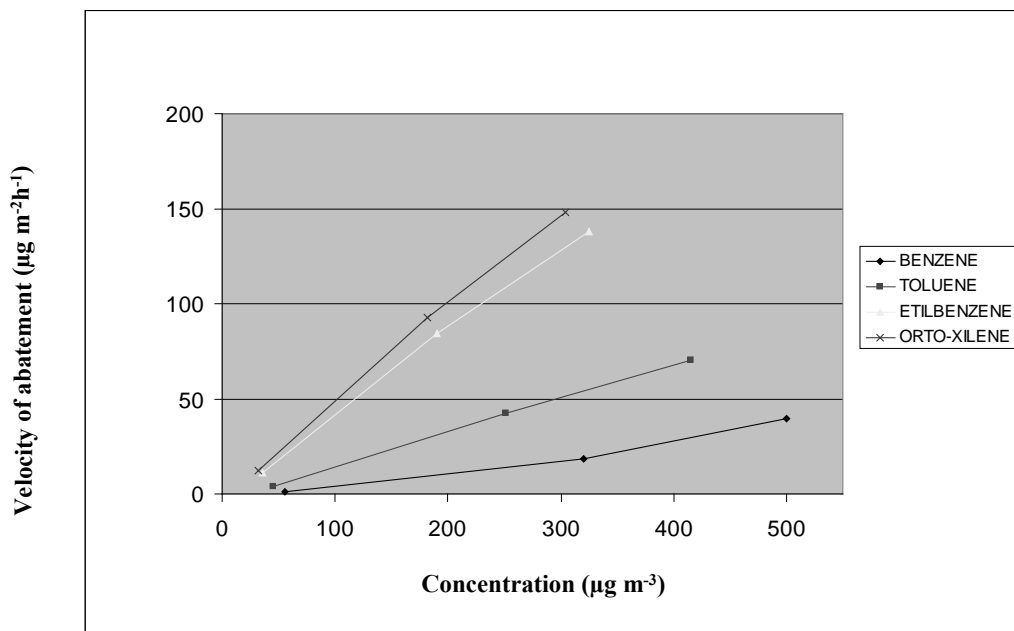


Fig. (31). Steady-State concentration of aromatics in vicinity of Eco-cement wall coating with a change in surrounding air velocity.

Annual Average Nitrogen Dioxide from Continuous Monitoring Sites (1999 - 2005)

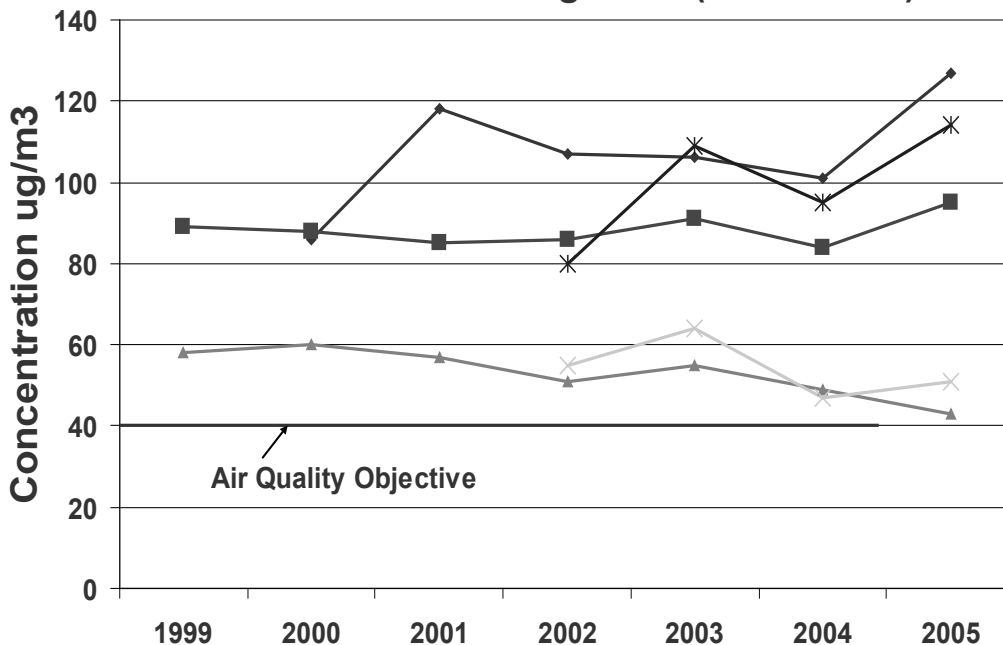


Fig. (32). Typical NO_x levels in different parts of London compared with actual safe (objective) levels.

ering.

It was therefore, ascertained that some 4.5 grams of NO_x gases were being removed daily by the paint. Also, calculations show that over the School surface some 10,000 m³ of air are

**Nitrate levels from the experiment carried out at the Sir John Cass School,
Aldgate London.**

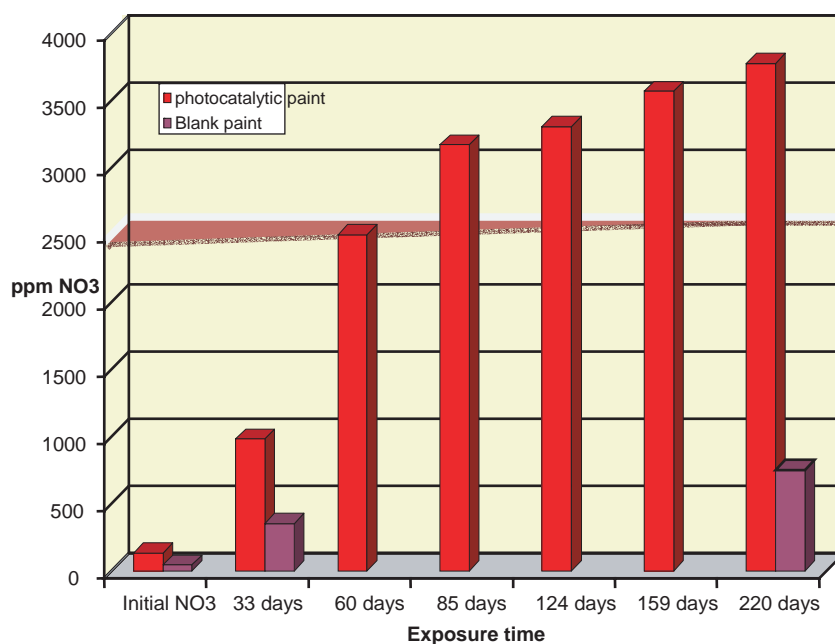


Fig. (33). Nitrate levels measured in trial coating experiments at a School in Aldgate London.

being cleaned each day which equates approximately, to some 2,000 cars passing by each day. Paving trials have also been undertaken i.e. in Saville Row, London and here Table 6 shows that typically NO_x levels are drastically reduced in areas where the photocatalytic fluids are being applied.

Table 6. Typical Pilot NO_x Levels Obtained in Trial Paving Experiment in Saville Row, London

Before application of Fotofluid	NO	85ppb
	NO _x	110ppb
	NO ₂	24ppb
After application of Fotofluid	NO	3ppb
	NO _x	8ppb
	NO ₂	5ppb

CONCLUSIONS

Photooxidation studies on paint films show a clear demarcation between nano-particle and pigmentary grade titanium dioxide with the former being more active. Model system studies based on 2-propanol oxidation and hydroxyl analysis go some way to predicting pigment activities but precise correlations do not always exist in the real world.

The use of nanoparticle anatase in conjunction with pigmentary rutile grades is also a viable option for the development of self cleaning paint surfaces. For antibacterial surfaces nanoparticles are effective whereas pigmentary grades are ineffective. Highly effective photocatalytic grades of nanoparticles can also be prepared through control of the preparation and subsequent drying operations.

The antibacterial activity of the nanoparticle pigments was inversely proportional to particle size, and relates to their intrinsic ability to generate active carriers giving rise to active surface species. Pigments calcined at higher temperatures, consequently with fewer structural defects, are more active, because defects act as recombination centres for the electrons and holes. Hence the antibacterial efficiency of TiO₂ is not determined by surface area but by the ability to generate active carriers resulting eventually in the formation of effective chemical species such as peroxides (hydrogen peroxide). This is not surprising because of the size of bacteria relative to the pigments: the majority of the surface area offered by a pigment is sterically unavailable to the bacterial cells. In terms of future building developments especially in the medical world this would offer significant advantages for eliminating the potential of MRSA. Current building work pilot trials show high efficiency in reducing fungal growth on for example, walls and roofing structures.

The paint coatings are also active to NO_x and VOC's, particularly once irradiated with UV with high levels of TiO₂ and CaCO₃ enhancing activity. This effect is associated with increased porosity of the paint system induced by both the titania and calcium carbonate particles. Unfortunately, higher levels of TiO₂ and CaCO₃ impart lower durability to the paint matrix. Higher levels of TiO₂ and CaCO₃ also reduce translucency of the paint films thus increasing absorptivity. On a positive note higher levels of CaCO₃ would react with more HNO₃. Nitrate compounds would be washed into the eco-system but levels are expected not to be harmful to the environment. For plant growth significant benefits would be expected.

Photocatalytic cementitious materials offer significant advantages from an environmental point-of-view on all issues associated with long term activity, durability, self-cleaning and de-pollution of NO_x and VOC's in various locations with air models showing high efficiency.

ACKNOWLEDGEMENTS

The authors would like to thank the PICADA consortium Global Engineering, Milan, Italy for the use of some of the data in this article.

REFERENCES

- [1] Murphy J. Additive for plastics handbook, 2nd ed. Elsevier 2001.
- [2] Patton TC. Pigment handbook Vol.1. J. Wiley & Sons, 1973.
- [3] Vesa DR, Judin P. Verfkroniek 1994; 11: 17.
- [4] Gurav A, Kodas T, Pluym T, Xiong T. Aerosol processing of materials. *Aerosol Sci Technol* 1993; 19(4): 411-52.
- [5] Balfour JG. Fine particle TiO₂, its properties and uses, Paper presented at SURCONY 91, New Mater 1992; 1: 21.
- [6] Allen NS, McKellar JF. Photochemistry of dyed and pigmented polymers, Applied Science Publishers Ltd., London, 1980; p. 247.
- [7] Allen NS, Edge M, Ortega A, Liauw C M, Stratton J, McIntyre R. Behaviour of nanoparticle (ultrafine) Titanium dioxide pigments and stabilisers on the photooxidative stability of water based acrylic and isocyanate based acrylic coatings. *Polym Degrad Stab* 2002; 78(3): 467-78.
- [8] Fujishima A, Rao TN, Tryk DA. TiO₂ Photocatalysts and diamond electrodes. *Electrochim Acta* 2000; 45: 4683-90.
- [9] Gao L, Zhang Q. Effects of amorphous contents and particle size on the photocatalytic properties of TiO₂ nanoparticles. *Scripta mater* 2001; 44: 1195-8.
- [10] Xu W, Zhu X, Fu X. The growth of TiO₂-X film and the quantum size effect studied by Uv-Vis spectroscopy, sem, tem and Ab initio calculation. *J Phys Chem Solids* 1998; 59(9) 1647.
- [11] Hoffmann MR, Martin SW, Choi W, Bahnemann DW. Environmental applications of semiconductor photocatalysis. *Chem Rev* 1995; 95: 69-96.
- [12] Anpo M, Shima T, Kodama S, Kubokawa Y. Photocatalytic hydrogenation of CH₃CCH with H₂O on small-particle TiO₂; size quantization effects and reaction intermediates. *J Phys Chem* 1987; 91: 4305-10.
- [13] Jang H, Kim S. Controlled synthesis of titanium dioxide nanoparticles in a modified diffusion flame reactor. *Mater Res Bull* 2001; 36: 627-637.
- [14] Ye X, Jin Y, Lie G. Proceedings of ICETS 2000-ISAM, October 11, Beijing, Session 3, 2000; Vol. 1: pp. 718-21.
- [15] Somorjai GA. Chemistry in two dimensions: Surface, Cornell University Press, Ithaca, NY 1981; p. 551.
- [16] Mills A, Morris S, Davies R. Photomineralisation of 4-chlorophenol sensitised by titanium dioxide: a study of the effect of annealing the photocatalyst at different temperatures. *J Photochem Photobiol A: Chem* 1993; 71: 285-289.
- [17] Chatterjee D, Dasgupta S. Visible light induced photocatalytic degradation of organic pollutants. *J Photochem Photobiol C: Rev* 2005; 6: 186-205.
- [18] Allen NS. Degradation and Stabilisation of Polyolefins, In: Allen NS, Ed. Elsevier Science Publishers Ltd., London 1983; Ch 8, p. 337.
- [19] Allen NS, Edge M. Fundamentals of Polymer Degradation and Stabilisation, Chapman and Hall, Chichester, 1992.
- [20] Kaempf G, Papenroth W, Holm R. Degradation processes In TiO₂-pigmented paint films on exposure to weathering. *J Paint Technol* 1974; 46: 56.
- [21] Allen NS, McKellar JF, Wilson D. Luminescence and degradation of nylon polymers: Part II: Quenching of fluorescent and phosphorescent species. *J Photochem* 1977; 7: 319-324.
- [22] Allen NS, Bullen D, McKellar JF. Luminescence properties and photoactivity of sulphate processed rutile (titanium dioxide) pigments in commercial polyethylene. *J Mater Sci* 1979; 14: 1941-1944.
- [23] Day RE. The role of titanium dioxide pigments in the degradation and stabilization of polymers in the plastics industry. *Polym Degrad Stab* 1990; 29(1): 73-92.
- [24] Allen NS, McKellar JF, Wood DGM. Photochemical processes involving titanium dioxide pigments and titanium dioxide-light stabiliser combinations in commercial polyolefins. *J Polym Sci Polym Chem Ed*, 1975; 13: 2319-25.
- [25] Allen NS, Gardette JL, Lemaire J. Interaction between titanium dioxide pigments and hindered piperidine/ antioxidant combinations in the photostabilisation of polypropylene. *Dyes Pigm* 1982; 3(4): 295-305.
- [26] Fujishima A, Rao TN, Tryk DA. Titanium dioxide photocatalyst. *J Photochem Photobiol Rev* 2000; 1: 1.
- [27] Bryk MT. Degradation of filled polymers, Ellis Horwood, London, 1991.
- [28] Pappas SP, Kuhhirt WJ. Photochemistry of pigments, UV curing and energy transfer. *J Paint Technol* 1975; 47(610): 42-8.
- [29] Voeltz HG, Kaempf G, Fitsky HG. Weathering of paints. *Prog Org Coat* 1972; 14: 1941.
- [30] Cundall RB, Rudham R, Salim MS. Photocatalytic oxidation of propan-2-ol in the liquid phase by rutile. *J Chem Soc Faraday Trans I* 1976; 72: 1642.
- [31] Boonstra AH, Mustaers CAHA. Relation between the photoadsorption of oxygen and the number of hydroxyl groups on a Titanium dioxide surface. *J Phys Chem* 1973; 79: 1694.
- [32] Kaneko M, Okura I, Eds. Photocatalysis: Science and Technology: Springer-Verlag GmbH & Co. KG, Heidelberg 2002.
- [33] Allen NS, Edge M, Sandoval G, Verran J, Stratton J, Maltby J. Photocatalytic coatings for environmental applications. *Photochem Photobiol* 2005; 81: 279-86.
- [34] Blake DM, Maness PC Huang Z, Wolfrum EJ, Huang J, Jacoby WA. Application of the photocatalytic chemistry of Titanium dioxide to disinfection and the killing of cancer cells. *Sep Purif Methods* 1999; 28(1): 1-50.
- [35] Kikuchi Y, Sunada Y, Iyoda T, Hashimoto K, Fujishima A. Photocatalytic bactericidal effect of TiO₂ thin films: dynamic view of the active oxygen species responsible for the effect. *J Photochem Photobiol A: Chem* 1997; 106: 51-6.
- [36] Sunada K, Kikuchi Y, Hashimoto K, Fujishima A. Bactericidal and detoxification effects of TiO₂ thin film photocatalysts. *Environ Sci Technol* 1998; 32: 726-8.

Received: September 11, 2008

Revised: September 19, 2008

Accepted: September 20, 2008

© Allen *et al.*; Licensee Bentham Open.

This is an open access article licensed under the terms of the Creative Commons Attribution Non-Commercial License (<http://creativecommons.org/licenses/by-nc/3.0/>) which permits unrestricted, non-commercial use, distribution and reproduction in any medium, provided the work is properly cited.